DETECTION OF EARLY STAGES OF DEGRADATION ON PPTA FIBERS THROUGH THE USE OF POSITRON ANNIHILATION LIFETIME SPECTROSCOPY

by

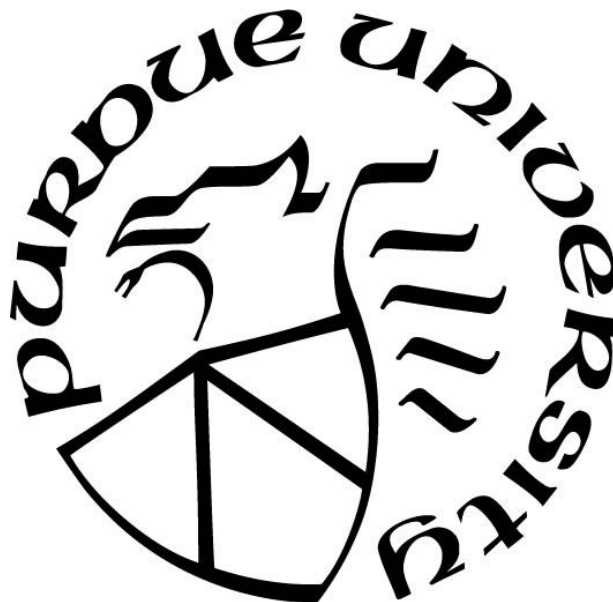**Nelyan López Pérez**

A Dissertation

Submitted to the Faculty of Purdue University
In Partial Fulfillment of the Requirements for the degree of

Doctor of Philosophy

School of Materials Engineering

West Lafayette, Indiana

August 2019

THE PURDUE UNIVERSITY GRADUATE SCHOOL
STATEMENT OF COMMITTEE APPROVAL

Dr. John A. Howarter, Chair

    School of Materials Engineering

    Environmental & Ecological Engineering

Dr. Kendra A. Erk

    School of Materials Engineering

Dr. Chelsea Davis

    School of Materials Engineering

Dr. Carlos Martínez

    School of Materials Engineering

Approved by:

    Dr. David F. Bahr

        Head of the Graduate Program

To Mami (Nélida Pérez De Hoyos) and Papi (David López Rivera), my parents. Thank you for all the music, singing, and French lessons. Thank you for letting me fill my mirror with equations. Thank you for all the times you used ice cream as a bribe to make me go home and take a break from studying. Thank you for supporting me to go to Germany on my own. Thank you for all your sacrifice, support, love and for allowing me and encouraging me to take opportunities that make me learn and grow. ¡Los amo!

To my sister Daneli López Pérez and her husband Andrés M. González Bonet, my brother José I. López Pérez and his wife Yaiza M. Santiago López. Thank you for your advice, for believing in me, but most of all, for leading the way.

To Viviana López Jiménez, my cousin and role model. Thank you for inspiring me to see the world and aspire to great things.

To my aunts Loyda, Awilda and Lucila, for the care packages and sofrito that reminds me of home.

To Adrián David González López, my nephew, my joy.

¡Infinitamente, gracias!

ACKNOWLEDGEMENTS

TABLE OF CONTENTS

LIST OF TABLES

LIST OF FIGURES

ABSTRACT

Author: López Pérez, Nelyan. Materials Science Engineering.
Institution: Purdue University
Degree Received: PhD. August 2019
Title: Detection of Early Stages of Degradation on PPTA Fibers Through the Use of Positron Annihilation Lifetime Spectroscopy.
Committee Chair: John A. Howarter

High-performance fibers used for ballistic protection are characterized by having outstanding mechanical properties such high modulus and strength. These mechanical properties are granted by the fiber's chemical and physical structure as well as their high degree of orientation. Twaron fibers are one of the most commonly used fibers on soft body armors such as bulletproof vests. They are made from poly (p-phenylene terephthalamide) (PPTA), a rigid-rod and highly crystalline polymer. Although these fibers are crystalline and have great mechanical properties, their performance can decrease when they are exposed to different degradation factors. Free volume is the unoccupied space between the polymer molecules. It is responsible for characteristics such as diffusion and viscosity. Hence, the free volume changes as the polymer degrades. This thesis focuses on the effects of sonication, pH changes, and sweat on the free volume of PPTA fibers.

A non-destructive technique known as positron annihilation lifetime spectroscopy (PALS) was used to measure the free volume in PPTA. Changes in the free volume of fibers degraded under different conditions were compared to their mechanical performance. Degradation in DI water, pH 4 and pH 10 aqueous solutions was conducted for 10 weeks at 80°C. Sweat degradation of PPTA fibers was also conducted for 10 weeks at 25°C, 50°C, and 100°C. Fibers degraded in pH4 and sweat solutions had greater loss of mechanical performance and changes in the free volume. PALS was able to detect changes in the nanostructure of PPTA fibers at early stages of

degradation. This data was supported by mechanical tests and is complementary to other characterization techniques such as small angle X-ray scattering (SAXS). Results of this research are a steppingstone for future studies on lifetime predictions of bulletproof vests and the development of the next generation of soft body armors.

CHAPTER 1   PPTA FIBERS

Some of the information include in this chapter was retrieved from Nelyan López Pérez's Master Thesis titled "Degradation Of High Performance Polymeric Fibers: Effects Of Sonication, Humidity And Temperature On Poly(P-Phenylene Terephthalamide) Fibers"[1].

1.1   Introduction

Since the beginning of humanity, protection form weapons have been essential for survival. Through history body armors have been constructed based on the materials available, the knowledge of materials, and the weapons available. For example, a medieval knight had a heavy armor made from several layers of metal, which mainly offered protection from stabbing. Perhaps this armor was efficient but not practical, flexible, or comfortable.

With the invention of the gun, other kind of body armor was created. Natural fibers, like silk, were used for the protection against bullets. The use of fibers for body armors offered more flexibility to the wearer. However, silk body armors were not efficient. The synthesis of polymers brought with it the possibility to make stronger fibers that would imitate the qualities of the natural fibers. One of them was Nylon, an aramid fiber. This polymer, commonly used for feminine stockings, was also used for body armors.

Research continued with the purpose to create stronger synthetic fibers. Among those fibers was Kevlar, created by accident by Stephanie Kwolek in DuPont[2]. Kevlar is composed of poly (p-phenylene terephthalamide) (PPTA) molecules. The synthesis of Kevlar as well as the spinning method used to produce the fibers was a breakthrough on the Chemistry, Polymer and body armor fields. Overall, the use of PPTA fibers like Kevlar on ballistic applications like soft body armors offer flexibility without compromising protection. We will this discuss this in more depth on the following sections.

Kevlar forms part of a classification of fiber known as high-performance fibers, which are crucial for many of today's tasks that involve heavy loads or performance under harsh conditions. This thesis will focus on one high-performance fiber known as Twaron (a PPTA fiber like Kevlar) and its performance as it is exposed to different conditions. Before we get into more details, it is important to know more about the fibers, their structure, and how they interact with their surroundings. But first it is important to understand what high-performance fibers are.

1.2   High-Performance Fibers

High performance fibers are fibers that have high mechanical properties like modulus and strength. Fibers with these characteristics can be made of materials such as: polymers, ceramics, metals and carbon. These fibers are engineered to be used harsh environments. Some examples of high performance fibers are glass fibers, which are commonly used for communications (fiber optics), insulation, and as a reinforcement in composites [3]. The scope of this thesis will cover polymeric high-performance fibers used for ballistic protection like soft body armors (e.g. bullet proof vests). Fibers used for ballistic protection are strong enough to absorb the kinetic energy of a bullet and the dissipation of the frictional energy [4].

Polymers used for high performance fibers can form crystalline domains and can be flexible or have rigid-rod molecules. The difference between flexible and rig-rod fibers is the technique that is used to produce them. Moreover, the mechanical performance of these fibers is greatly due to the orientation of the polymer molecules in the fibers[5].

1.3   Structure of PPTA Fibers

As mentioned before, the mechanical and chemical properties of PPTA fibers, depend on the molecular structure and composition of the polymer structures. PPTA fibers are part of group

of fibers known as aramids. Aramids are composed by 85% of amide groups which are bonded to aromatic rings[2]. The position of the bonds between the amide group and the aromatic ring makes a difference on the ability of the molecules to form hydrogen bonds (h-bonds). **Figure 1.1** compares m-aramid (*meta*-aramid) molecules to p-aramid (*para*-aramid) molecules (PPTA). The para position makes easier the formation of H-bonds than the meta position.
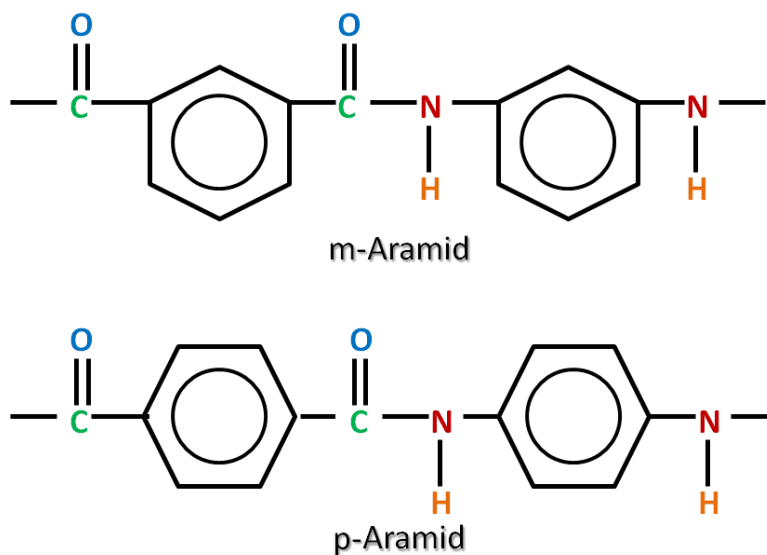
Figure 1.1 Molecular structure of m-aramid and p-aramid polymers

The formation of hydrogen bonding allows greater degree of crystallinity. PPTA molecules can stack with each other (as seen on **figure 1.2**) and form the crystalline domains. The presence of the aromatic rings on the backbone grants the PPTA molecules rigidity, whereas the amide groups allow the formation of H-bonds. Since crystallinity reduces the space between the molecules, crystalline domains are resistant to chemical attacks. Overall, PPTA fibers possess covalent bonds within the backbone and H-bonding as the principal intermolecular bond.
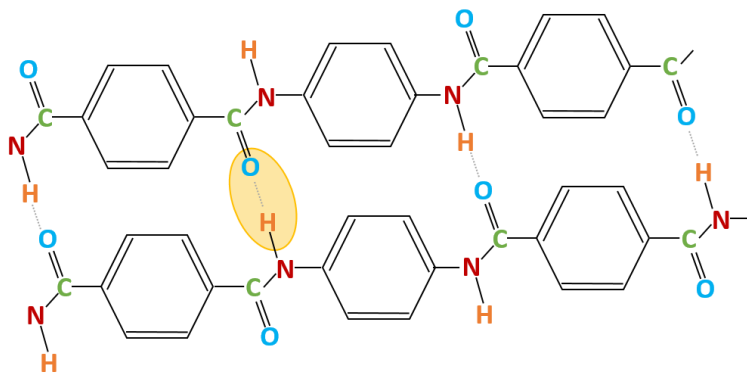
Figure 1.2 *Stacking of PPTA chains by H-bonds between the molecules.*

The physical structure of PPTA fibers is created through the spinning process by which they are produced. Some fibers are produced by melt spinning or "dry spinning", a process on which the polymer is melted and extruded through a spinneret [6]. PPTA fibers cannot be made through this process, since they are too rigid and degrade before they reach their melting temperature. Instead, PPTA fibers are made through a process known as "dry-jet wet spinning". This process consists of the dissolving the polymers in sulfuric acid (H_2SO_4) which forms a liquid crystal polymer (LCP) solution [7]. This method allows the polymer to be extruded at a lower temperature than its melting temperature, prevents premature degradation, and allows greater order in the fibers. The concentration of polymers in solution ranges from 10% wt. to a limit of 20% wt. in order to have a nematic liquid crystal solution[4][8].
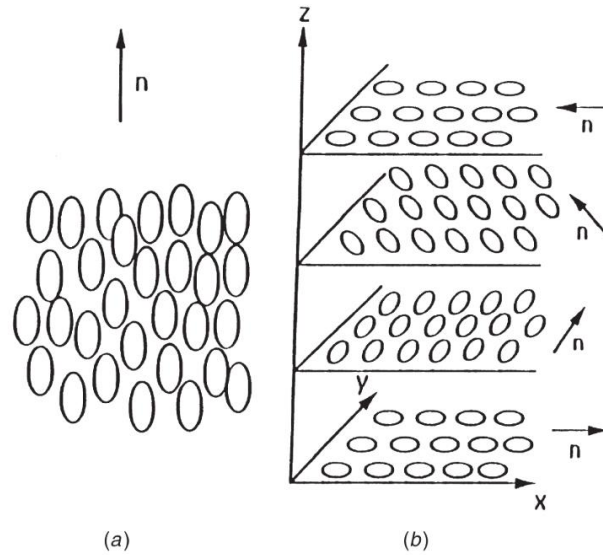
Figure 1.3 *In the nematic phase (a) crystal domains are randomly position but they are aligned on the same direction. Cholesteric phase or chiral (b) cosists of different planes. Each plane has a different direction of alignement. A helical structure is formed* [9].*Retrieved from Khoo, I., Liquid Crystals.*

A nematic liquid crystal has global alignment of the crystalline domains but there is no specific order between each particular domain (as seen on **figure 1.3**)[10][9]. Each crystalline domain is composed of the aligned PPTA molecules. When the polymer is extruded the crystalline domains of the LCP align and become more ordered. After extrusion, the fibers go through a coagulation bath, which removes the excess of the solvent and allows the polymers to relax. At this point a gradient on the orientation of the crystalline domains forms in fibers as they cool down. **Figure 1.4** shows the synthesis and dry-jet wet spinning process of Twaron fibers[11]. As a result of the dry-jet wet spinning process, different structures are formed within the fiber.
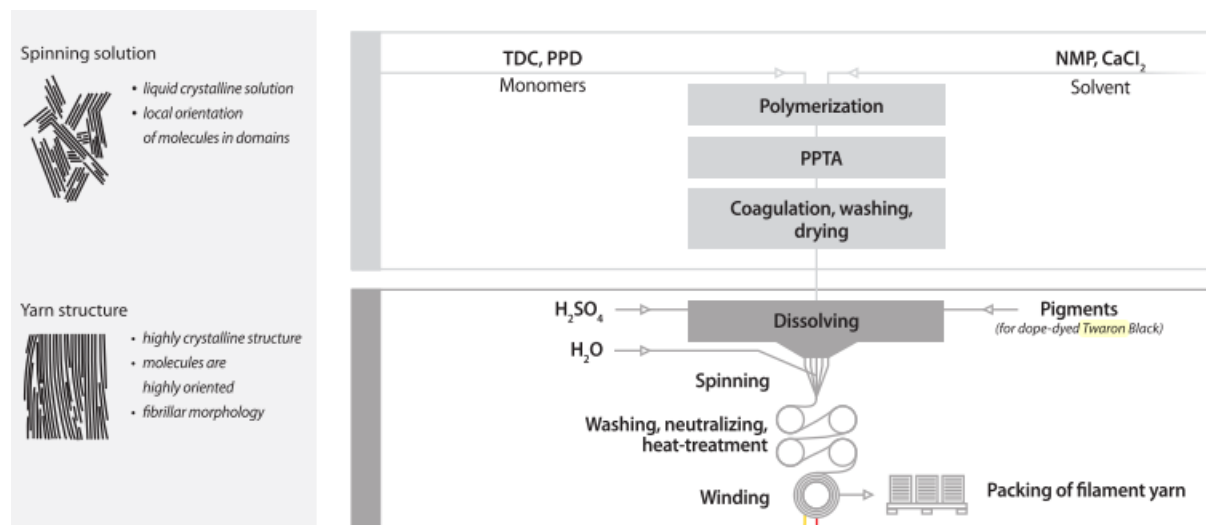
Figure 1.4 *Synthesis and spinning process of PPTA fibers. This image was retreived from the Teijin Twaron brochure* [11].

i. *Skin-core structure*

When the fibers are extruded, the domains closer to the spinneret are quickly aligned and cooled (since they are at the surface). On the other hand, the crystalline domains at the center of the fiber are "relaxed" and they have more time to move and change their orientation until they completely cool and reach their final position[4]. This forms the core of the fiber and, due the relaxation process described before, it is composed of more chain defects, chain ends, and voids[2]. **Figure 1.5** is a schematic by Morgan et al. that describes the difference between the skin and core of PPTA fibers[12].
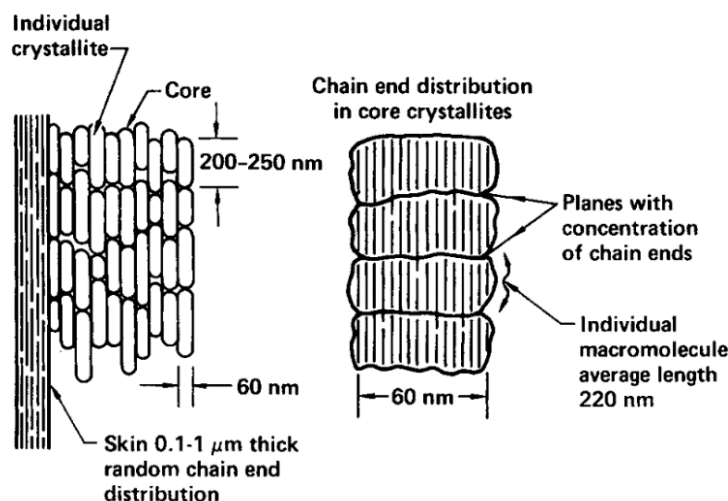
Figure 1.5. *Skin-core structure of PPTA fibers. Retrieved from Morgan et al.* [12]

ii. *Fibrils*

According to D. Ahmed et al., fibrils are "crystalline threadlike entities"[2]. They are formed by sheets of aligned and extended PPTA molecular chains that are bonded to each other through H-bonds. The sheets are bonded with van der Waals forces. Fibrils are found all through the fibers but differ if they are in the skin or at the core. In the skin, fibrils are uniformly oriented to the fiber axis, whereas the fibrils at the core are imperfect on their orientation [2].

iii. *Pleated structure*

Pleats are formed by oriented crystals that are parallel to each other. They are oriented in a way so that the axis at which the h-bond between the PPTA molecules occur is perpendicular to the surface of the fiber[2].
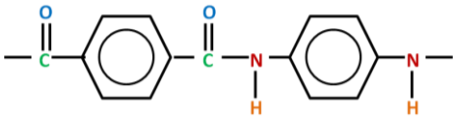
1.4   **Mechanical Properties of PPTA Fibers**

Table 1.1 shows the values of different mechanical properties of Twaron PPTA fibers[11]. The modulus and tensile strength of Twaron is similar to the mechanical properties other high-

performance fibers like ultra-high molecular weight polyethylene (UHMWPE) and carbon fibers. As mentioned before, these properties are attributed to the crystallinity of the fibers and taking advantage of having covalent forces along the fiber axis.

Table 1.1 Mechanical properties of PPTA fibers

Chemical Structure	Modulus (GPa)	Tensile Strength (GPa)	% Elongation	$T_{degradation}$ (°C)
	60-120	2.4-3.6	3.0-4.4	500

Compared to UHMWPE, Twaron and other PPTA fiber can retain more moisture (due to polarity). However, PPTA fibers can be used to a wide range of applications, since their degradation temperature is high. For example, UHMWPE melts at around 144°C while Twaron decomposes at 500°C and does not melt. This characteristic is attributed to the high crystallinity of the fibers and the presence of aromatic rings in the PPTA molecules.

1.5   **Fiber-Water Interaction**

Although PPTA fibers are highly crystalline and resistant to chemical attacks, the presence of water can affect their mechanical performance[13]. Humidity is present on the daily use of soft body armors in different forms: sweat, weather conditions, storage conditions, etc. Other factors that contribute to the absorption of water on PPTA fibers is the presence of residual hydrophilic salts form the spinning process[14].

PPTA fibers like the Twaron fibers used for the purpose of this research, retain 3-5%wt. of water[11]. This moisture can be found as two kinds: loosely bound and tightly bound water. The

latter is bound to the crystal lattice and requires more energy to be desorbed. Studies on the moisture in Kevlar 49 revealed that 6% of the water present in the fibers is loosely bound, while 30% is tightly bound[15].

In semi crystalline polymers diffusion of water occurs in the amorphous areas. These areas also prone to chemical attacks. PPTA fibers do not possess amorphous areas, but they do have defects and chain ends are areas on which water can diffuse[16].The most accurate computational model that describes the moisture sorption process in PPTA fibers is the intercalation model.
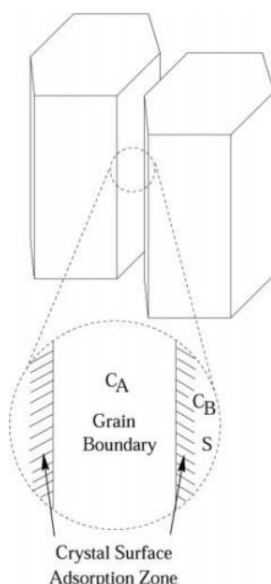
Figure 1.6 *Grain boundary regions and absorption zone described by the intercalation model. This image has been retrieved form Mooney et al. [15].*

The intercalation model considers two regions: an "amorphous" region and a crystalline region. The former consists on the grain boundaries between the PPTA crystallites and the latter considers the crystallites[17]. According to this model, water diffusion occurs on the amorphous regions and interacts with the surfaces of the crystalline domains (see **figure 1.6**) [17]. Other studies done by J. Wang et al. also propose the formation of water layers between the PPTA crystallites[18]. They observed that at low relative humidity PPTA fibers have higher creep

activation energy than at higher relative humidity. Therefore, they concluded that a monolayer of water is stronger than multi-layers of water between the crystallites (see **figure 1.7**).
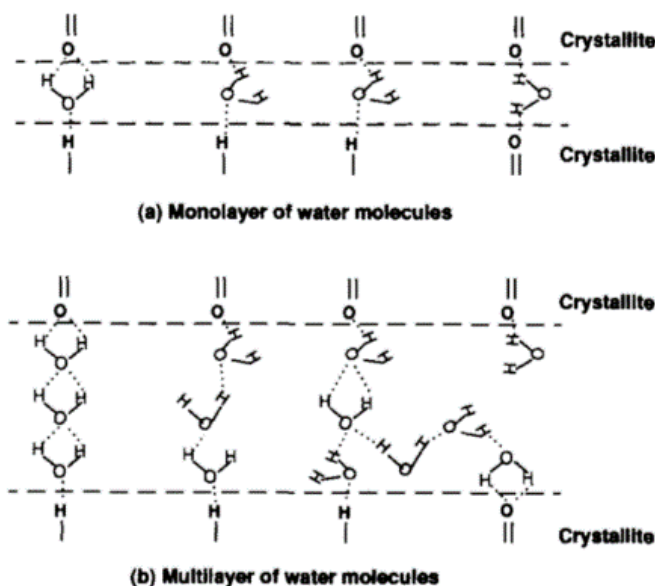
Figure 1.7 *Water molecules between PPTA crystallites. Image retrieved from J. Wang et al. [16]*

The formation of water layers between the PPTA crystallites influences the mechanical performance of the fibers. When water is introduced to the fibers, hydrogen bonds are formed, as seen of **figure 1.7**. The presence of multilayers of water allows the crystallites to slide when a stress is applied[18]. Hence, it is important to study the effects of water on the mechanical properties of PPTA fibers over time.

1.6   **Tensile Testing and Fracture of PPTA Fibers**

Tensile testing is a very straight forward characterization technique through mechanical properties of a material can be acquired. Through this method, a stress versus strain curve of the material is plotted as the sample under study is stretched in one direction[19] . The results of the plotted stress-strain curve show how much elastic and plastic deformation the material undergoes

until it fails and breaks. Ductile materials like the semicrystalline material represented in red in **figure 1.8**, have and initial elastic response. This means that if the applied load is removed, little to no deformation is done. If the material is stretched even further, it will reach a point where plastic deformation takes place known as the yield point. In the case that the material is stretched even more, it will reach its ultimate tensile strength. This point indicates the maximum load that the material can support without breaking[20]. After reaching this point, a semicrystalline material will experience a wider amount of strain at a lower stress than the ultimate tensile strength. Later on, the stress will increase at a higher rate until it the material breaks and fails.

Ballistic fibers possess high crystallinity and will exhibit a brittle behavior such as the green plot in **figure 1.8**. In this case, the ultimate tensile strength and the fracture point are the same. This is one of the properties that are measured in this project along with the elastic modulus. The latter is determined with the slope of the stress-strain curve.
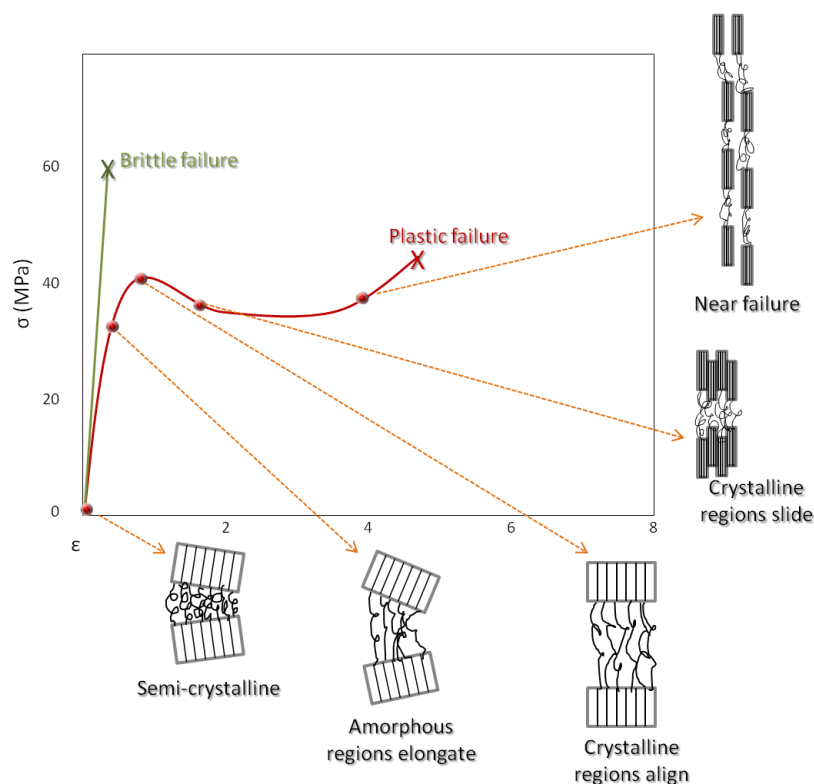
Figure 1.8 *Stress-strain curve of a brittle material versus a plastic semicrystalline material. Effects on the microstructure of the semicrystalline material is shown step by step as it is deformed. This figure is adapted from[19]: Callister, W. D. Materials Science and Engineering: An Introduction.*

Figure 1.9 shows a stress vs. strain curve of a PPTA yarn sonicated for two hours in water and shows a brittle response when subjected to a tensile load. This is due to the high orientation of the polymer chains and crystallinity. Fracture of these fibers mainly consist of chain-scission which is more likely to initiate at the chain-end and defects [21]. Said defects do not only affect the failure, but also contribute to the deformation and strength of the fibers[2][12]. Fracture in highly oriented fibers like PPTA occur by crack propagation that produce an axial split break[22]. These fibers, as mentioned in previous sections, have a higher molecular strength in the axis in which the fiber was drawn than between the molecules.
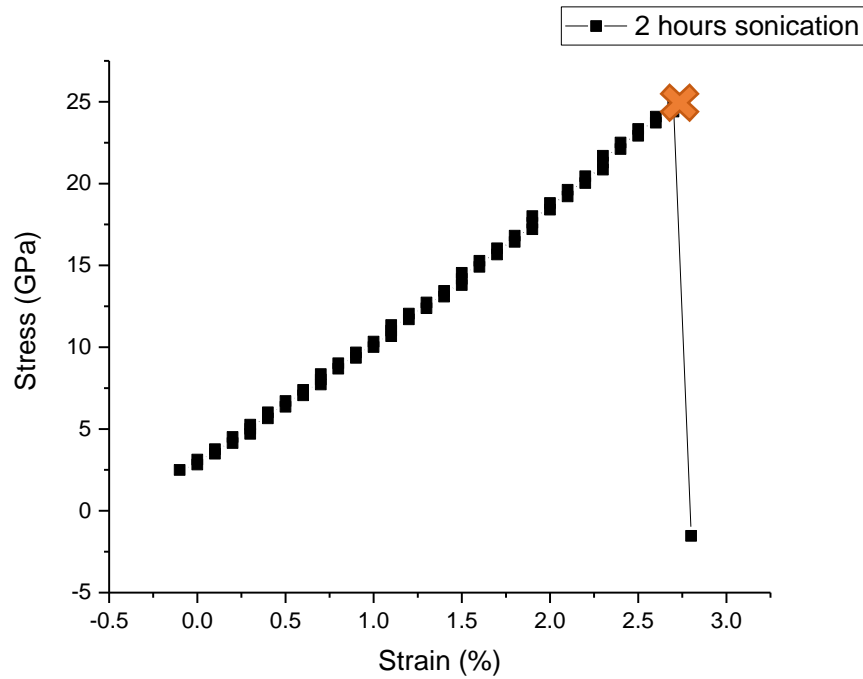
Figure 1.9 *Stress vs. strain graph of a PPTA yarn degraded in pH 4 for 6 weeks. The shape of the curve is the same for all the yarns tested. The ultimate tensile strength (UTS) is marked by the x.*

Failure in PPTA fibers mainly consists in crack propagation. Cracks are formed as a consequence of the breakage of hydrogen bonds between the chains as the fiber experiences tension. In the core, the propagation follows a transverse path along the sites where there are chain ends[12]. As it reaches the skin, the path follows a transversal and lateral propagation marked by the difference in the structure between the two areas as seen in **figure 1.10**.
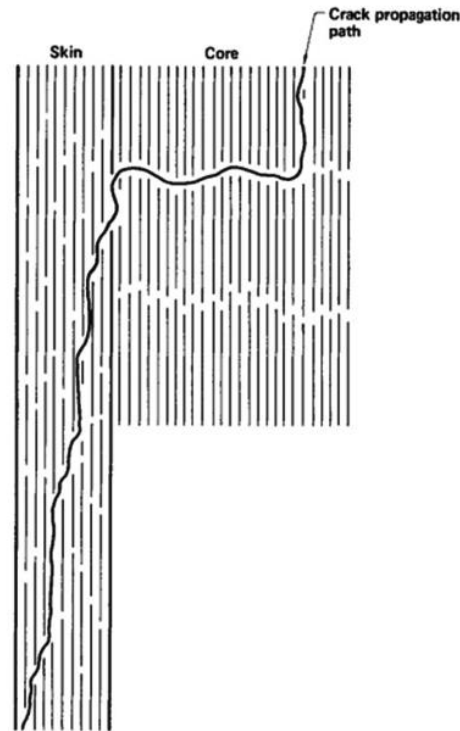
Figure 1.10 *Crack propagation model proposed my Morgan et al[10],[1].*

1.7   **Degradation of PPTA Fibers**

Degradation is the reduction of a material's properties[20]. Moreover, it is a process that occurs over time and at every stage of the life of a material. In their processing stage, PPTA fibers are exposed to high temperatures, stress and solvents. These factors can introduce impurities and defects in the fibers[23].

Through the lifetime of use of body armors, PPTA fibers are exposed to humidity, sweat, changes in temperature, sunlight and wear. Each of these factors also contribute to the reduction of the fiber's mechanical properties. The reason for this reduction on the material's performance relies on changes on the chemical or physical structure of the fibers as a consequence of being exposed to the factors mentioned before[20][23].

The chemical structure of a fiber, or a material in general, determines how it will interact with its surroundings. For example, a molecule's polarity will indicate if it is soluble or prone to

be attacked by certain chemicals. On the other hand, tacticity, the order at which a polymer is arranged[24], contributes to the flexibility of the polymer molecule. In the case of PPTA, tacticity is one of the factors that influences crystallinity, due to its "para" (p) conformation[25].

Crystallinity also plays an important role in how a fiber will interact with its surrounding. Polymers are more susceptible to chemical attacks on amorphous regions[20][26][27]. This is because there are more space available and bigger molecules can interact with the polymers. On the other hand, crystalline areas are densely packed and prevent the interaction of foreign molecules.

Exposures to some of these environmental factors can lead to chain scission or crosslinking. In both cases, the mechanical properties of the material are altered. Chain scission consists of breaking chemical bonds and results in the reduction of the polymer's molecular weight. Contrary to chain scission, crosslinking creates bonds and increases the molecular weight. Degradation initiates in weaker sites. In the case of PPTA fibers, these sites include microvoids, chain ends and defects. Chain ends are areas where the stress concentrates and they transfer the load to adjacent chains[28]. As a consequence, the strength of the crystallites is lowered[28].

Changes or over exposure to humidity may provoke a hydrolytic reaction. Hydrolysis is a chemical reaction that involves the rupture of a molecule into two smaller molecules. One of the molecules that are a product of this reaction is attached to a hydrogen atom obtained from water and the other molecule is attached to an –OH group[29] .

As mentioned in previous sections, the crystallinity of PPTA fibers contribute to the resistance to water and chain scission due to hydrolysis but water can still be adsorbed in the system[13][17]. A higher degree of hydrolysis in PPTA occur in an acid or basic environment since these extreme pH degrees act as a catalyst to the hydrolytic reaction[30] (see **figure**

1.11).Residues of acid or base chemicals can remain in the fibers after synthesis and can affect the performance of the fibers during the use stage.
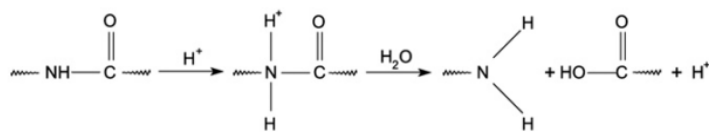
Figure 1.11 *Proposed mechanism of hydrolysis of Kevlar in the presence of acid [25], where a carboxylic acid group and an amine group are a product. Taken from Arrieta, C. et al. Hydrolytic and photochemical aging studies of a Kevlar-PBI blend.*

Moreover, hydrolysis can take place when fibers are exposed to deionized water and high temperatures. Their degradation rate under these conditions increase with temperature[31]. Changes in the surface morphology after weeks have been found, as well as the appearance of small voids (~10Å) which could be initiation sites for hydrolysis and the breakage of tie points as seen on **figure 1.12**.
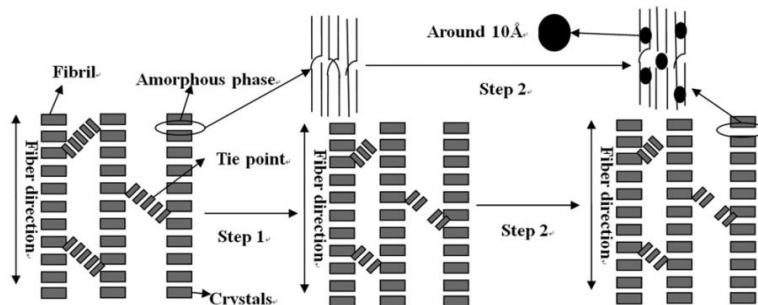
Figure 1.12 *Possible mechanisms of hydrothermal aging of Kevlar. Degradation occurs on the amorphous regions of the fiber [26]. Retrieved from: Li,C.S. et al.*

On the next chapters, we will be discussing in more details the methods of degradation studied on this thesis. The first method of degradation that will be presented will be sonication and how it affects the creep behavior, sorption and mechanical performance of PPTA fibers. The

second study discussed on this thesis focused on the effects of DI water, pH 4 and pH 10 aqueous solutions at temperatures higher than room temperature. Furthermore, the effects of sweat at different temperatures were also studied for this thesis. For each method of degradation, the mechanical performance of the fibers was compared to changes on the nanostructure of the fibers. Changes in the nanostructure, specifically the free volume, were measured

CHAPTER 2   POSITRON ANNIHILATION LIFETIME SPECTROSCOPY

This chapter will cover one of the basic concepts of polymeric materials known as free volume and how it is measured through positron annihilation lifetime spectroscopy (PALS). Knowledge of how PALS data and how it is related to the change in the structure of polymers can be used to describe the effect of degradation in fibers like PPTA. Parts of this chapter are acquired from the submitted paper "Free Volume - Performance Relationship of PPTA Fibers: Accelerated Degradation in Sweat, Acid, Basic and Neutral Aqueous Solutions". SAXS data and analysis was done in collaboration with Jessica Sargent.

2.1   Free Volume in Polymers

All polymers have a specific volume, which is the inverse of their density. The specific volume is used to determine the crystallinity of a polymer by methods like the Archimedes' method and measuring the density gradient[27]. Moreover, the specific volume is the sum of a polymer's crystalline and amorphous volume fractions.

Temperature affects the specific volume. **Figure 2.1** shows the trend of the specific volume on a semi-crystalline polymer as temperature increases. Notice that there are two regions: glassy and rubbery. In the glassy phase, the molecules have little motion, therefore, the slope at this phase is less steep than at the rubbery phase. At the rubbery phase, polymers have more freedom to move and the slope of the line changes to be steeper. The point at which the two slopes intersect is known as the glass transition temperature. Moreover, the value of each slope is the coefficient of thermal expansion. The reason why there is such as difference in the slopes is the presence of free volume in the material.
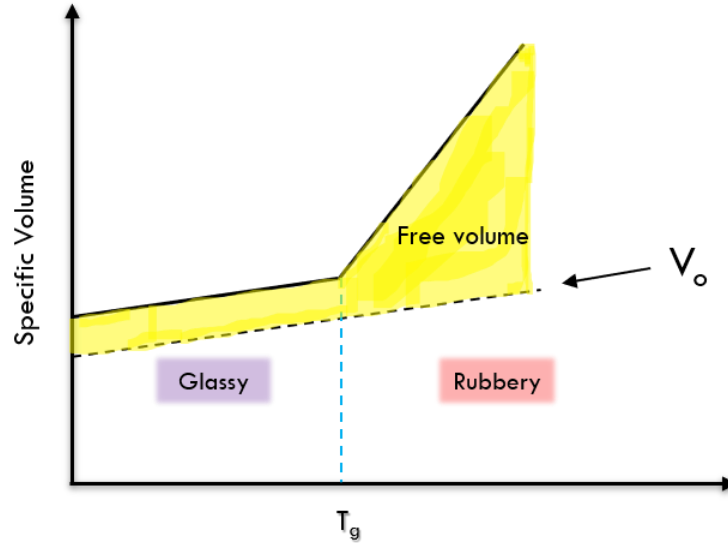
Figure 2.1 *Sketch of the change in specific volume of a polymer as temperature increases.*

Free volume is the space that is not occupied by polymer chains, or the empty space between polymer molecules. The dimensions of the free volume depend on the polymer's crystallinity and external factors such as temperature[27]. This free space influences properties such as the viscosity, diffusion of molecules, and the physical aging of a polymeric material[32][33]. The free volume (V_f) is related to the specific volume (V_{sp}) with the following mathematical relationship[32]:

$$V_{sp} = V_f + 1.3V_W$$

V_W is the value of the van der Waals free volume, which is the volume occupied by the polymer molecules. The van der Waals volume cannot be penetrated by other molecules at a normal range of thermal energies[34][35]. The constant 1.3 is an approximation of the ratio of the crystalline volume to the V_W at 0K [35].

Since the free volume is essential to determine the viscosity and the diffusion of a polymer, different stages of a polymer's degradation process are also determined by changes in the

dimensions of the free volume. In the following sections, a non-destructive method that is used for the measurement of the free volume is discussed in more detail.

2.2   **Free Volume and Positrons**
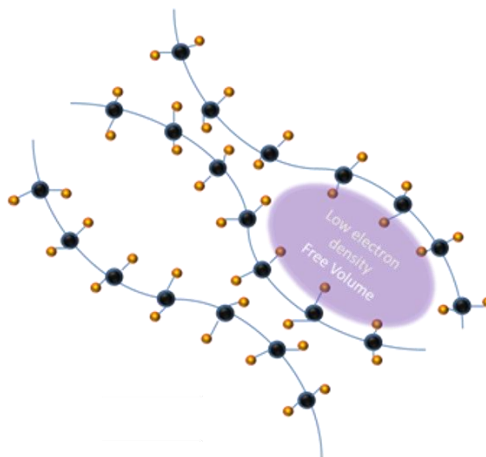
Figure 2.2 Sketch of the free volume/low electron density areas on polymers.

Free volume in a material is an area that has low electron density (**figure 2.2**). In nature, there is a particle that is likely to reside in these areas. Said particle is known as a positron (e^+). A positron is the antiparticle of an electron, having its same mass but different charge as the electron. When a positron encounters an electron, it forms a new particle called a Positronium[36] (see **figure 2.3**). When this bound state annihilates it can do so in one of two states: para (p-Ps), where spins are anti-parallel, or ortho (o-Ps), where the spins of the particles are parallel to each other [36][37] .
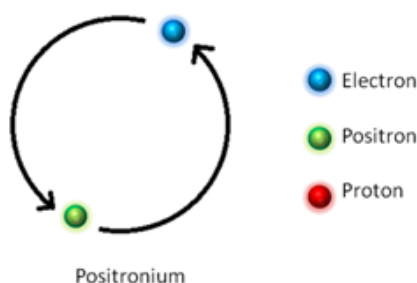
Figure 2.3 Sketch of a positronium. This image was adapted from Principles and Applications of Positron and Positronium Chemistry by Y. Jean et al [36].

Each of the bound states has a different lifetime. In vacuum p-Ps has a lifetime of 0.125ns and o-Ps has a lifetime of 142ns (**figure 2.4**) [36]. However, the lifetime of these particles varies on the material. Most importantly, the lifetime of these particles is related to the size of the free volume. The relationship between the lifetime of the positron and the size of the free volume will be explained in section 2.3.
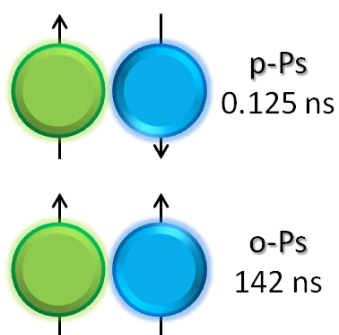
Figure 2.4 Sketch of the spins and lifetimes of positronium. This image was adapted from Principles and Applications of Positron and Positronium Chemistry by Y. Jean et al[36].

2.3   **Positron Annihilation Lifetime Spectroscopy**

The interactions of positrons with matter is the basis of a technique that can measure the free volume in a material. This technique is known as Positron Annihilation Lifetime Spectroscopy (PALS). This method measures the energy of the photons emitted when a positron is released and

when the annihilation with an electron occurs. PALS detects this energy and measures the time between these two events. This amount of time is considered the lifetime of the positron (emission to annihilation). The time that it takes from the emission of the positron to the formation of the positronium is considered the lifetime of the positronium[38][37]. **Figure 2.5** shows a sketch of the PALS set up and how it measures the lifetime of the positron[39]. In the sketch, PM is a photodetector and SCA is a single channel analyzer. There are two of each because one detects the start signal (release of positron ~1.27 MeV) and the other one detects the stop signal (annihilation ~511 keV). TAC is the time-to-amplitude converter, which is attached to the multichannel analyzer (MCA) [39].
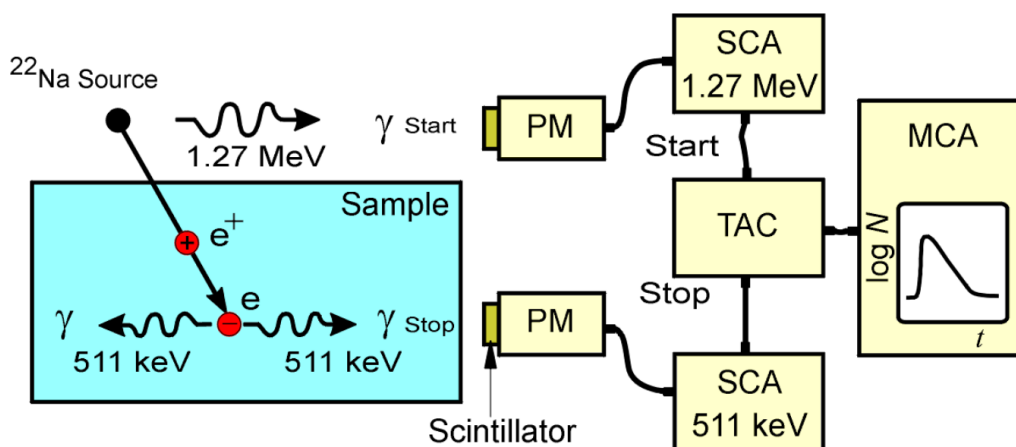
Figure 2.5 *Sketch of the PALS setup and how it measures the lifetime of positrons by detecting the energy of photon that are emitted when a positron is released and when it annihilates with an electron and form a positronium [9].*

Two important parameters are acquired using this method: the lifetime and the intensity of the particles. The lifetime of the o-Ps (τ_3) is related to the radius of the free volume. The amount of free volume with the dimensions determine by τ_3 is the intensity. PALS takes advantage of the positron-matter relationship, and with the use of the Tao-Eldrup equation (**Equation 1**), the radius (R) of the free volume can be measured[37].

$$\tau_{o-Ps} = C \left[1 - \frac{R}{R + \Delta R} + \frac{1}{2\pi} \sin \frac{2\pi R}{R + \Delta R} \right]^{-1} \otimes M$$

Equation 2.1. *Tao-Eldrup equation.*

In this equation $R + \Delta R$ is also considered R_0, which is based on a spherical quantum well model[40], is the radius of an infinite spherical potential well[37] [41]. R is the hole radius and ΔR (0.1656 nm) is the electron layer between R_0 and R ($\Delta R = R_0 - R$) [42]. The constant C is the intrinsic positron/positronium lifetime (for polymers it ranges from 0.5 to 2[34][43]) and $\otimes M$ is a function that compensates for any modifications of the spherical structure and the polymer chemistry. Assuming that there is no chemical interaction between the polymer molecules and the positrons (no destruction of the molecules, and only interaction with the free volume), the value of $\otimes M$ is equal to 1[37]. Considering all these constants, in order to know the radius of the free volume in PPTA fibers, we solve for R.

The value of R calculated from equation 1, along with the intensity of the o-Ps (I_{o-Ps}), are used to calculate the free volume of the material. Equation 2 shows the calculation of the fractional free volume (V_f) assuming that free volume areas are spherical ($V_f = \frac{4}{3}\pi R^3$). According to Y. Yu, the minimum dimensions detected by PALS are radius of 0.13 nm and volumes of 0.0092nm^3 (I_{o-Ps}= 1%) [33].

$$Fractional\ V_f = \frac{4}{3}\pi R^3 * I_{o-Ps}$$

Equation 2.2 *Calculation of the fractional free volume of a material.*

PALS data can be described as a Gaussian distribution that can be deconvoluted into three sub distributions, one for each resolved lifetime. Each lifetime corresponds to a type of annihilation. In polymers τ_1 corresponds to p-Ps annihilation and has a value of 0.125ns, $\tau_2 \sim 0.45$

ns corresponds to positron annihilation (free positrons). The last lifetime value $\tau_3 \sim$ 1-5ns corresponds to o-Ps annihilation, and it has information of the free volume sites in the material. The latter is the lifetime used in the Tao-Eldrup equation.

2.4 **The Use of Pals in Previous Studies**

PALS has been used as a method to determine the glass transition temperature in polymers[44], and the gas permeation ability of polymer membranes[45]. A more recent study used PALS to determine how the free volume changes as cellulose nanofibril films swell when exposed to different degrees of humidity[46]. In said study, initial adsorption of humidity in CNCs is reflected as a decrease in free volume, since the latter is now occupied with water. Further results indicate that at higher relative humidity (RH) levels the pores/free volume expands. This is noticed when the lifetime and radius of the free volume increase. The study also revealed that as humidity increases, more free volume is created, which is noted by an increase in the intensity of the signal. Cellulose nanofibrils are hygroscopic, which means that they can absorb water, a characteristic also found in PPTA fibers.

A study that confirmed the behavior of free volume as polymers physically age was conducted by D. Bigg et al. concluded that in fact greater positronium lifetimes were detected in amorphous polymers and amorphous areas of semi-crystalline polymers[41]. In other cases, PALS has been implemented before in studies of the effect of humidity on polyimide membranes that are used for gas separation and insulating applications[47].

Specific studies of PALS on PPTA fibers have been conducted by J. Howarter et al. focused on the effects of physical aging through folding [48]. They compared PPTA to other high-performance fibers like poly(p-phenelyne-2,6-benzoxazole) (PBO) commercially known as Zylon and fibers made from PBIA-*co*-PPTA (a PPTA copolymer). It was concluded that PPTA fibers

had little to no change on their mechanical performance and pore size after 80,000 folds. However, PBO and PBIA-*co*-PPTA had a significant reduction on their mechanical performance and increase in the pore size and intensity of the free volume present in the fibers after 80,000 folds[48]. Moreover, PALS is a non-invasive technique that can measure the size and amount of free volume in materials. Nonetheless, it should be used as a complementary technique to methods such as small angle x-ray scattering (SAXS), by which more detailed information about the crystallinity and structure of the material can be acquired.

SAXS, like other X-Ray tests, measures the crystallinity of materials like polymers based on the diffraction pattern that results from the interaction between the incident radiation and the material at certain angles. The angles used in this technique are from 1° to 5°[49]. Compared to PALS, which can measure free-volume areas (through the lifetime of o-PS) of around 0.3-0.7nm, SAXS can measure structures ranging from 0.7-50nm[49]. This characterization method has been previously used on single biopolymer fibers[50], as well as for the determination of the structure morphology of Kevlar[51] and electrospun fibers[52].

Overall, PALS is a technique that offers a less invasive method of characterization, since it studies bulk material, whereas SAXS can determine the crystallinity of a single fiber. Acquiring information from both techniques, enables a broader and detailed understanding of the structure of PPTA fibers as they degrade.

Once again, this research aims to use PALS along with mechanical characterization methods to relate the changes in the mechanical properties of PPTA fibers with the dimensions of the free volume as they age. By doing this, early signs of degradation can be detected and an estimate of the lifetime of the fibers can be calculated.

2.5 **Data Collection and Experimental Setup**

Samples used for PALS are required to be at least 2mm in thickness. This is because that

is the penetration depth of the positrons in a material[38]. The system used for the research

discussed in this thesis was an ORTEC PLS-SYSTEM which is a complete positron annihilation

picosecond timing system[53]. A Na^{22} positron source (POSK-22-10 from Eckert & Ziegler) was

used for all experiments. The latter had 10µC of activity and 2 years of half-life 950.8 days (2.60

years)[54].

For each PALS run two samples of the condition were required to cover the Na^{22} source.

Figure 2.6 shows how the sources is sandwiched between the two samples and pressed with the

detectors.
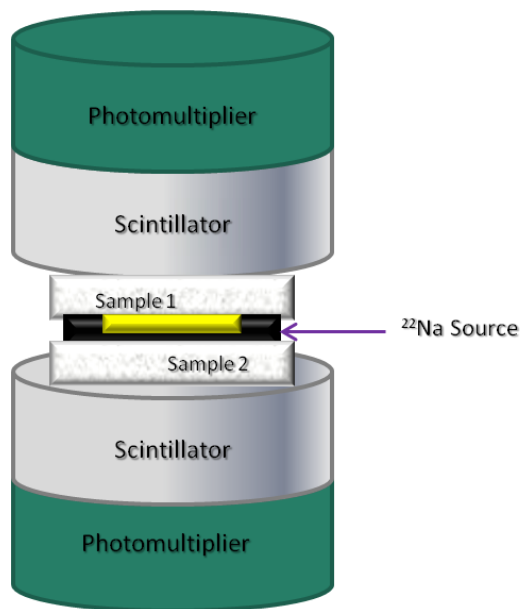
Figure 2.6 *Sketch of the PALS setup. Sample 1 and sample 2 are PPTA samples.*

The software used for the detection of the positrons was Maestro, provided by Ortec. In

order to have a good fit runs required a minimum of a million counts. This translates to 3-4 days

for polymers, depending on the age of the source.

2.6   **PALS*fit* Software and Data Analysis**

The curves acquired through the Maestro software is analyzed with another software called PALSfit. PALSfit is a program made by Peter Kirkegaard, Jens V. Olsen, Morten Eldrup, and Niels Jørgen Pedersen from the Risø campus of the Technical University of Denmark[55]. This software creates a model function that fits the data collected through Maestro. The model function is the sum of exponential decays that are convoluted with a time resolution function and includes a constant background [55]. This software is based considering least square fitting. PALSfit is used in two modes: ResolutionFit and PositronFit. ResolutionFit records positron lifetime spectra to determine the time resolution function of the spectrometer [55][56]. On the other hand, PositronFit used data from the ResolutionFit to measure the spectra in terms of the proposed model function and extract the lifetimes and intensities of the positrons in the materials[55][56].

It is important to notify that there is no "user friendly" software guide or academic article that explains how to use PALSfit. Therefore, indications included in this thesis on how to use PALSfit are based on the user experience through the years of this research.

Figure 2.7 shows the main components of the PALSfit interface. The red lines (outer lines) determine the range of the area of the spectra, while the green lines (inner lines) determine the fit minimum and maximum. The blue line (middle line) determines the time-zero channel. The x-axis represents the channels and y-axis represents the number of counts per channel. The time scale of our system is 0.012860ns/channel, which was determined by the calibration of the PLS-SYSTEM by Ortec.
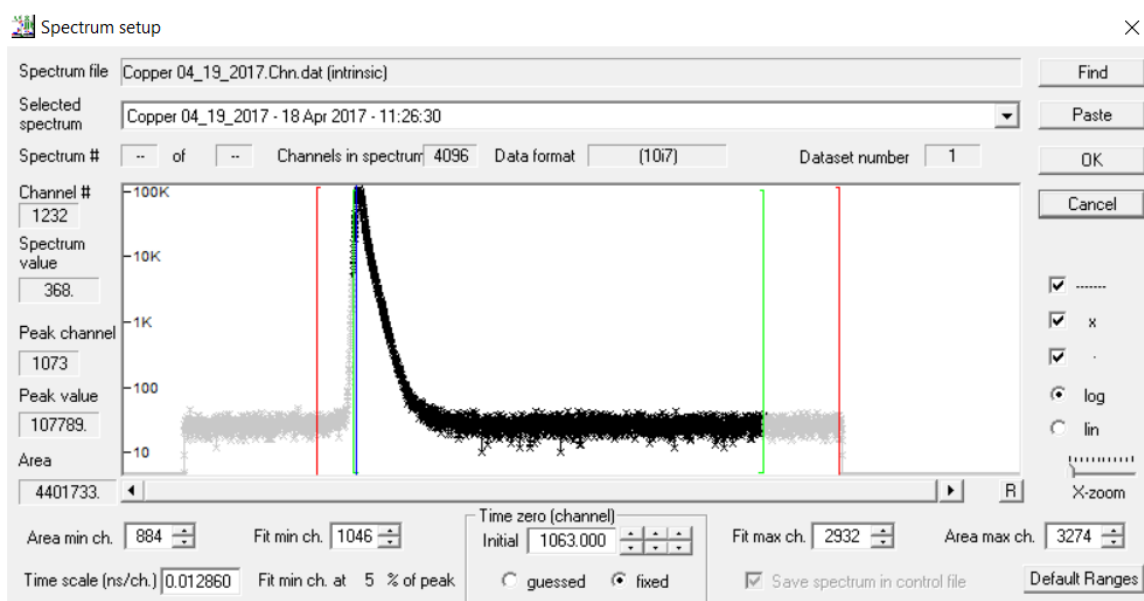
Figure 2.7 *Screenshot of a PALS spectrum on PALS fit and the parameters for analysis.*

Samples of annealed copper are used to obtain the resolution function through ResolutionFit. To obtain a resolution, guesses of the intensities (%), the half width at half maximum (FWHM), and the lifetimes had to be made. Also, a background is selected. Analysis of the ResolutionFit are made and guesses are changed depending on the value of the reduced chi-square (which should be ~1) and the significance of imperfect model. According to Jens V. Olsen et al. a good resolution function is acquired when the values of the FWHM , lifetimes and intensities remain constant with any change [55]. Once the resolution function is obtained, the values of the FWHM and shifts on the fits of the gaussian decays are used on PositronFit to make the analysis of the different samples.

PositronFit has a similar procedure. Three lifetimes where used for both ResolutionFit and PositronFit. The lifetimes guessed were: 0.125ns, 0.4ns, and 1ns. The 0.125ns lifetime accounts for "free positrons", 0.4 considers the lifetime contributed by the Kapton film that encases the Na^{22} salt, and 1ns is the guessed value of o-Ps. The value of the reduced chi-square and the significance

of imperfect model are changed and improved when the "Fit min" and the "Time-zero" values are the same.
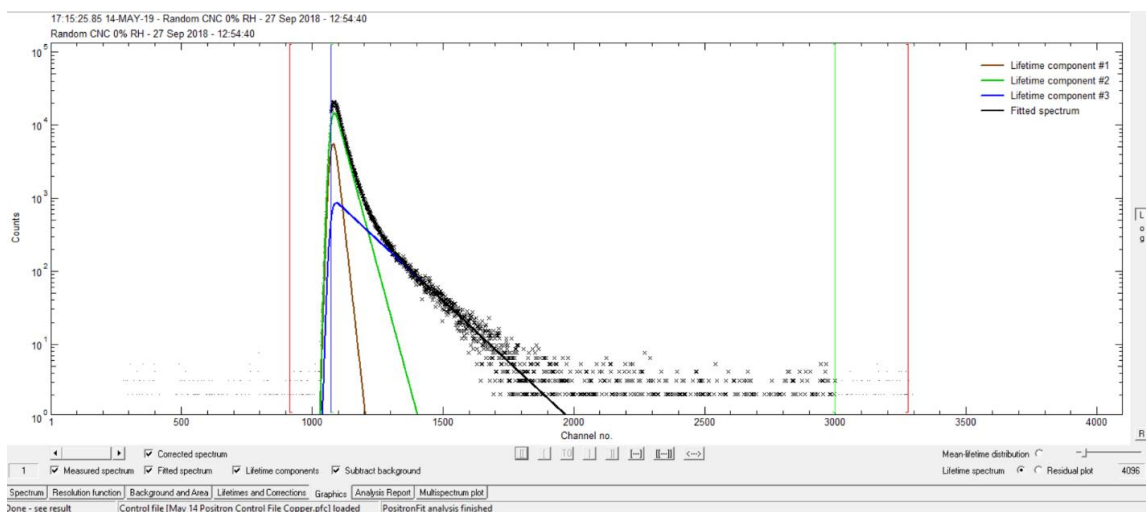
Figure 2.8 Screenshot of the "Graphics" tab on PositronFit mode of PALSfit. This example is taken from a CNC sample.

Figure 2.8 shows a screen shot of the "Graphics" tab on the PositronFit mode of PALSfit. This tab allows you to see the different gaussian decays considered to extract the different lifetimes. Lifetime component #3 is used for the lifetime of the o-Ps since it is the longest. This also considered the tail of the curve. However, not all the data from the tail is useful. To know which channels to discard on the fit, "Residual plot" on the right corner of the "Graphics" tab is selected. **Figure 2.9** is an example of what is found on the "Residual plot". A "structured" pattern is seen at around channel 1800 and above. Changing the value of the "Fit max" to channel 1800 improves the fit. More than one "good fit" can be found for each spectrum.
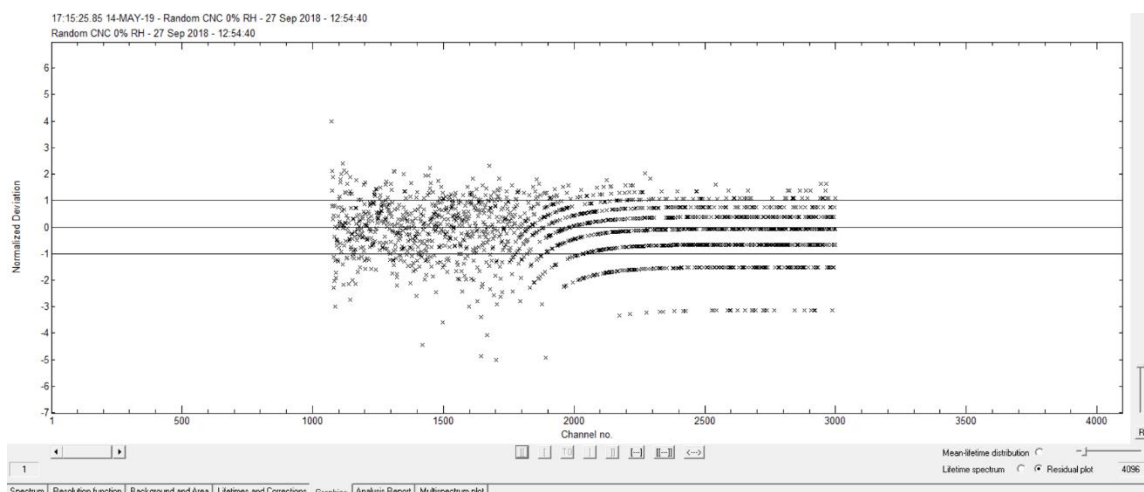
Figure 2.9 *Screenshot of the residual plot of the PALS spectrum of a CNC sample.*

Since more than one good fit can be found, the strategy used for the purpose of this thesis was to consider the values of the o-Ps lifetime and intensities of the channels 1500 to 2000. **Figure 2.10** is an example of an analysis report. Analysis reports for each sample were saved and the values found (specifically on the lifetime and intensity of the 3rd lifetime) were used the Tao-Eldrup equation.

Figure 2.10 Screenshot of the analysis report of the fitting of the spectrum of a PPTA sample degraded in 0.1% of sulfuric acid (H2SO4) in water.

The software Origin was used to make Tao-Eldrup equation calculations. The Tao-Eldrup equation is transcendental and therefore, it is divided in two parts: sinusoidal and "linear". The linear component included the lifetimes extracted from the PALSfit analysis, and the value of the radius (R) is varied from 0 to 1 on the x-axis. Both the sinusoidal and the lineal parts of the equation (y-axes) are plotted again the radius (x-axis) as seen on **figure 2.11**. The x-value of the intersection of the curves is considered the radius attributed to that lifetime.
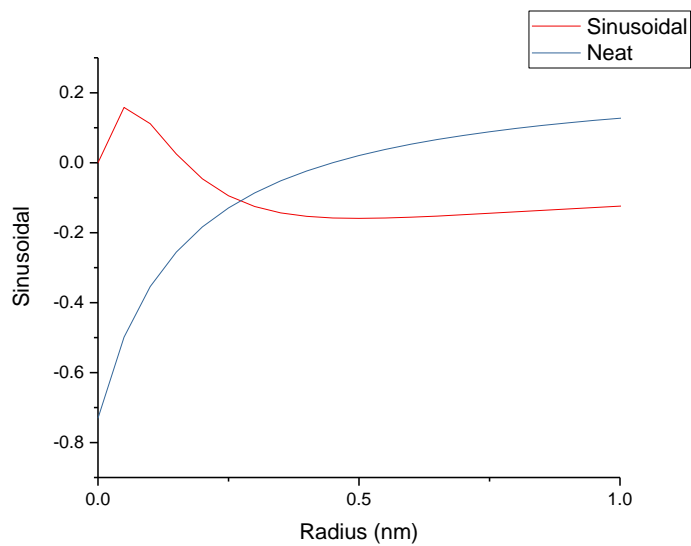
Figure 2.11 *Plot of the Tao-Eldrup transcendental equation. The value of x at the intersection of the two curves is the radius attributed to the lifetime.*

The data found through the calculation of the Tao-Eldrup equation for each degradation method studied for the purpose of this thesis will be discussed in chapters 3 and 4.

CHAPTER 3   SONICATION

Some of the information found in this chapter was previously discussed in Nelyan López Pérez's master thesis titled "Degradation of high-performance polymeric fibers: Effects of sonication, humidity and temperature on poly (p-phenylene terephthalamide) fibers"[1]. *More detailed information about this topic is found on that thesis. This chapter also contains information from the paper "Effect of Sonication on the Strength and Humidity Absorption of PPTA Fibers" in collaboration with Jessica Sargent. Furthermore, this chapter will discuss the effects of sonication on PPTA fibers and who it affects the creep behavior, humidity adsorption, and mechanical performance at different temperatures.*

3.1   **Introduction**

Poly (p-phenylene terephthalamide) fibers used for body armor applications are exposed to environmental factors, such as humidity and temperature, that contribute to their degradation. Due to their high-risk applications, it is important to study the degradation process of these materials to avoid their early failure during service. In order to mimic the aging process of these materials different methods of accelerated degradation are commonly performed on the fibers. The scope of this project involves using sonication to degrade the fibers, since it creates a harsh environment that causes tearing of the material and the formation of kink bands.

The determination of the amount of degradation the material undergoes is measured by mechanical characterization methods such as dynamic mechanical analysis and testing to failure. Sonicated fibers were studied at different percentages of relative humidity and temperatures, and the instant effect on their creep behavior and changes in mechanical properties such as the elastic modulus and the ultimate tensile stress were measured. Mechanical properties were compared to changes in the free volume and structure of the fibers by using positron annihilation lifetime spectroscopy (PALS) and small angle X-ray scattering (SAXS) respectively.

Results show that sonication hinders the effect of fatigue and increases the toughness of PPTA fibers. However, the presence of water in the environment increases the creep and, at longer

periods of time, it counteracts the strength acquired through sonication. These effects are of a greater magnitude at temperatures near room temperature.

3.2   **Sonication**

One of the drawbacks of studying the degradation process is that it takes years, which is not practical on a laboratory setting. Therefore, methods to accelerate this process are required to mimic the damage created through years of use but in a shorter time. In this research, we suggest sonication as a method for accelerated degradation. When a material is immersed in a sonication bath it experiences the following phenomena:

1. **Cavitation:** formation, growth and collapse of bubbles. This occurs due to the compression and rarefaction of the liquid. Vaporized liquid and gas are carried inside these bubbles[57].

2. **Localized high temperatures:** The system can experience temperatures up to 5000K[58].

3. **Localized pressure gradients**: Up to 1000 atm.

The magnitude of the effects of these phenomena are controlled by parameters such as the frequency and intensity of the ultrasonic waves, the solvent (quality, vapor pressure), molecular mass of the polymer and the external temperature and pressure. Consequently, sonication may result in intermolecular tearing and scrubbing of the fiber's surface[59]. Therefore, sonication creates a harsh environment in which the immersed fibers can suffer alterations in their structure. Visible signs of degradation after sonication such as kink bands and fibrillation have been previously detected and serve as proof of the effects of sonication[60]. Kink bands are a result of compressive loading that initiate shearing of the chains. On the other hand, fibrillation is the axial split of fibrils (loss of interfibrillar bonds) caused by abrasion[61]. Hence, sonication can be

considered a degradation method that can induce damage that may mimic the years of use but on a shorter time scale.

Although sonication can damage PPTA fibers, a study from Andrassy et al. suggested that it has positive effects on the fibers by reducing the aging tendency due to ultraviolet (UV) light exposure[62]. These results seem contradictory to the idea of using sonication as a degradation method, yet it is an opportunity for new research that aims to investigate if the same beneficial results can be obtained considering other factors such as humidity and temperature instead of UV radiation.

Humidity is crucial for PPTA fibers due to the hygroscopic and polar nature of the molecules that form it. This factor along with temperature alter the creep rate of the fibers and consequently their failure point. The goal of this project is to study the effects of sonication on PPTA fibers and its impact on their moisture absorption at different temperatures. Our approach includes mechanical tests that measure the creep response and failure of PPTA fibers as well as other methods that allows us to characterize their physical and chemical structure.

This study is a steppingstone for future work that will help the improvement of existing ballistic materials as well as the development of new ballistic materials and the prediction of their lifetime by recreating early stages of degradation.

3.3   **Materials and Methods of Characterization**

3.3.1   *Sample Preparation*

PPTA woven fibers (CT 709 Twaron fibers, provided by Teijin) were submerged in a beaker full of deionized water. Said beaker was submerged in a Bransin Ultrasonics (Branssonic model CPX 3800) ultrasonic bath with frequency of 40kHz. The fibers where sonicated for 2 and 6 hours. Fiber yarns were air dried and prepared for DMA testing. To maintain the fibers of the

yarn together, a thin layer of epoxy glue was deposited at the ends of the yarns. Epoxy was allowed to set for 24 hours. Another set of samples of woven PPTA were sonicated in hexane (Sigma Aldrich), to compare the effects of a polar and a non-polar solvent on the creep behavior of the fibers.

A humidity chamber was built to humidify neat and sonicated fibers for 24 hours at a constant temperature (30°C) and humidity (~50% RH). Samples humidified using this method were tested to failure.

Samples of 2cm x 2cm of neat, neat-water immersed, and 2-hour sonicated in water fibers were weighed, as they were neat, pat dried, and oven dried for 20 minutes at 80°C. The purpose of this test was to know the effects of sonication in water absorption.

3.3.2   Characterization

Scanning electron microscope (SEM) images were taken using the XL40 FESEM from Philips. Images of the neat and sonicated fiber yarns were taken to detect any visual signs of degradation like fibrillation or kink bands. Fibers tested to failure were also examined.
Neat, sonicated, and humidified fibers were tested to failure in an MTS Insight tensile tester (electromechanical-100kN standard length) with a load cell of 1000 N. A fiber fixture was used to test the fibers following the ASTM D 2256 standard[63]. Tape was adhered to the ends of the fiber yarns to prevent slipping.

Three tests were conducted using a DMA Q800 from TA Instruments (with a film fixture), which consisted of creep cycles under different conditions. Each test began with an initial force of 0.01 N and was ramped until it reached 18 N. The force was then held constant for 10 minutes. The latter was the amount of creep time, which was followed by an instant force decrease to the initial 0.01N.

1. *Humidity ramp test:* Measure the effects of humidity on PPTA fibers. The overall test consisted of 5 creep cycles, and each cycle was conducted at a different relative humidity. The first cycle was tested under 0 % RH, the second at 50% RH and the third at 80% RH. The following two cycles were 50% RH and 0 RH%. Temperature was kept constant at 30 and 60°C.

2. *Cycle-humidity test:* Measure the effects of fatigue and extreme changes in humidity. The test consisted of six creep cycles. The first three cycles were tested at 0% RH. After this series of cycles, the humidity was increased to 80% RH at which the last three creep cycles were tested. Tests were carried out isothermally at 30°C.

3. *Long Creep test:* Measure the long-term effects of sonication on the creep behavior of PPTA fibers. Moreover, it aimed to measure the effects of a polar and a non-polar solvent based on the assumption that hydrogen bonds can be formed between the PPTA crystallites and increase creep. Test consisted of only one creep cycle that was held for 2 hours and a constant humidity of 0% RH. Only sample yarns sonicated for 2 hours were tested.

PPTA woven samples were sonicated for 2 and 6 hours, pat dried and dried in an oven at 100°C for an hour. Two samples of the same degradation condition were used for each PALS run. Each run consisted on a million counts or more, to be able to have a good fit using PALSfit.

Small angle x-ray scattering (SAXS) can be used to characterize material structure and long-range order at the nanoscale. SAXS measures the scattering of a focused x-ray beam off of electron clouds in the material, where the intensity and angle of scattering is dependent on the density of electrons around a molecule and its arrangement relative to neighboring species. In this way, a measurement of the average size and orientation of various structural features of a material

can be obtained. At wider angles (i.e., shorter scattering distances), the size and orientation of crystalline domains within the PPTA fibers can be resolved.

SAXS measurements were conducted on neat fibers and fibers sonicated for 2 and 6 hours using an Anton Paar SAXSpoint2.0. Three frames of data for were collected for each sample and averaged to reduce signal contribution from environmental scattering. Data was collected at a scattering distance of 79 mm using an incident x-ray beam of 50 keV and 1.0 mA with a wavelength of 1.54 Ắ. 2D scattering patterns were reduced using SAXS Analysis software (Anton Paar) and normalized by sample transmittance.

3.4 **Results and Discussion**

3.4.1 *Water Absorption*
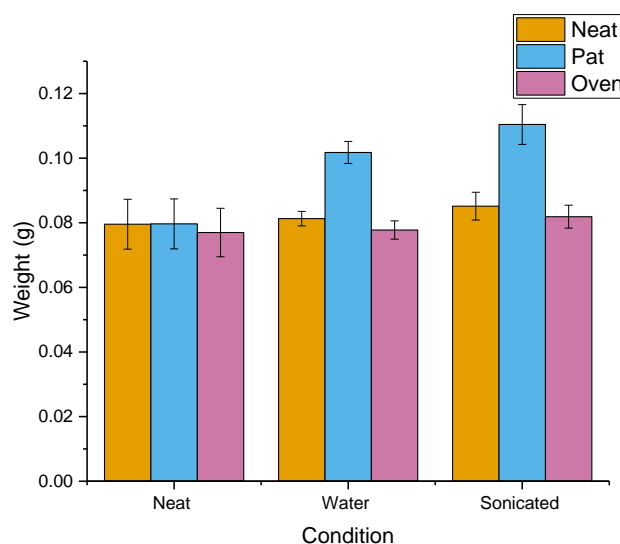
Figure 3.1 *Water sorption of neat, water immersed-neat, and 2-hours sonicated woven fibers.*

Data for the water absorption is plotted in **figure 3.1**. Neat fibers showed a reduction of 3% in weight after an hour of drying at 100℃. The slight change in weight is attributed to

desorption of pre-existing water in the fibers. When neat PPTA fibers were immersed in water and pat dried, their weight increased by 25%. Once they were dried in the oven, their weight was reduced to a lower value than at the initial neat weight.

On the other hand, sonicated fibers had a higher water uptake. After they were immersed in water and pat dried, they increased their weight by 30%. After they were dried in the oven their weight was reduced to a value lower than when they were neat.

3.4.2 SEM Images

Degradation signs are usually determined using microscopy and Fourier transformation infrared spectroscopy (FTIR spectroscopy). However, no visuals signs of degradation nor chemical changes were found using optical microscopy or FTIR respectively. Scanning electron microscopy is a more powerful technique to obtain visual evidence of degradation, and it was used in this project.

Images obtained for fibers sonicated for 2 and 6 hours are similar (**figure 3.2a**). They all show signs of fibrillation as revealed in **figure 3.2b**. Other signs such as kink bands were found in the sonicated fibers (**figure 3.2c**), which are a result of compression. These images follow the same trend found in previous studies. Failed fibers after the tensile testing experiments were also studied with SEM. **Figure 3.2d** demonstrates these fibers indeed failed in a fibrillar manner.

Although they are an indication of degradation, visual signs are not sufficient to determine the mechanical performance of the fibers. Hence, mechanical testing was performed.
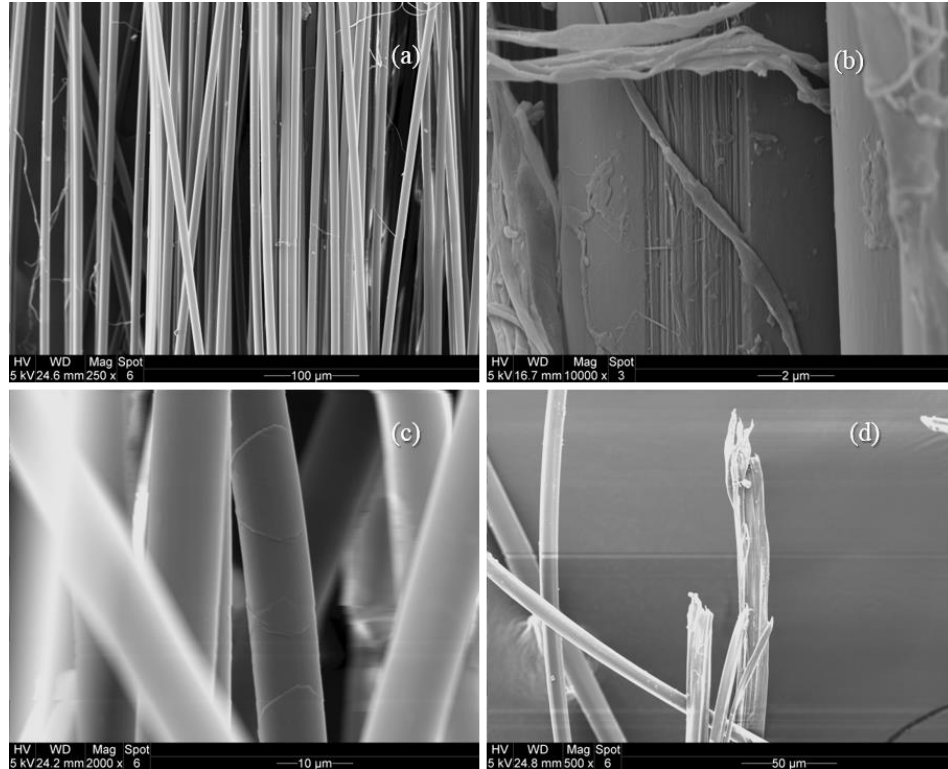
Figure 3.2 *(a) Sonicated PPTA fibers. (b) Evidence of fibrillation. (c) Evidence of kink bands.*
(d) Fibrillar failure of PPTA fibers.

3.4.3   Dynamic mechanical analysis

<u>Humidity ramp test:</u>

The amount of creep the fibers experienced during the test was calculated by subtracting

the final strain on every creep curve to the initial strain at 0% RH. The results were plotted in

figure 3.3.
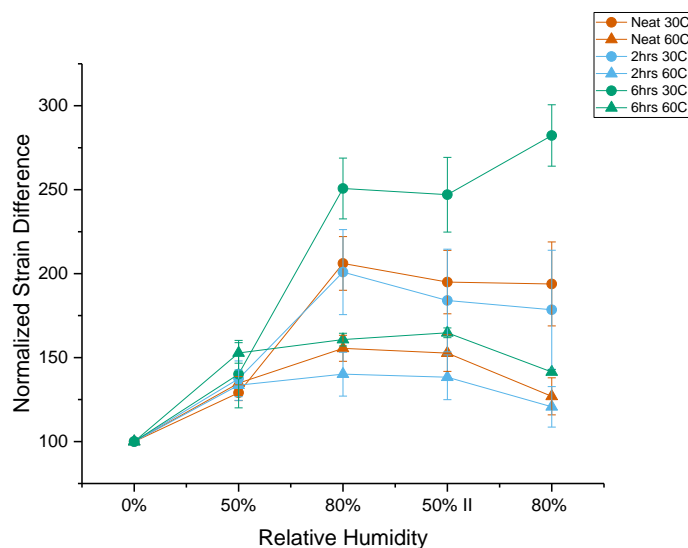
Figure 3.3 *Normalized strain difference of neat, and sonicated fibers for 2 and 6 hours and their response to relative humidity.*

A noticeable difference is seen between the creep behavior at 30°C and at 60°C. At 30°C all samples show greater strain than at 60°C. At 30°C, the strain increases as the relative humidity increases. Once the system reaches 80% RH the strain plateaus regardless of the decrease in relative humidity that followed. The difference in the behavior due to the temperature is similar to the results of previous studies made by Fukuda et al., where the moisture regain of Kevlar 49 fibers decreased as temperature increased[64]. In their work on the moisture sorption mechanism of aromatic polyamide fiber, it was concluded that the reduction of moisture sorption as the temperature decreased was due to the exothermic nature of the process, similar to the behavior of hydrophilic fibers such as rayon and nylon[64]. They used the BET multilayer adsorption model on isothermal curves of Kevlar 49 with changing relative humidity to support their conclusions. According to their results, the maximum volume of adsorbed moisture in a monolayer (v_m) and the adsorptive energy factor (C) decreased as the temperature increased.

Other theories attribute the reduction of the capacity of adsorption on fibers to the formation and destruction of crosslinks[65]. When the fibers are dry there are crosslinks and the latter are destroyed by the presence of water. As the water is removed the crosslinks reform. However, when the fibers are dried first, more crosslinks are formed, and the adsorption decreases. Hence, we see more adsorption at lower temperatures than at higher temperatures.

Therefore, at 60°C the moisture gained by the fibers was less than at 30°C. The increment in creep at higher relative humidity can be related to the formation of layers of water between the crystallites. At low relative humidity, monolayers of water molecules are formed between the crystallites due to the ability of PPTA molecules to form hydrogen bonds[18]. As more water is introduced to the system, more layers are formed, hydrogen bonds break and reform as **figure 1.7** illustrates[18]. The latter enables more mobility and consequently more creep to be observed.

The strain at 60°C was lower than at 30°C, but instead of reaching a plateau, it reached a maximum strain at around 80%RH and 50% II RH. However, the strain sharply decreased when the humidity decreased back to 0%RH.

Cycle-humidity test:

This test consists of two parts: fatigue at 0%RH and at 80%RH. In both cases the strain increased after each cycle. Under each relative humidity condition, the strain increased slowly after each cycle, yet there was a sharp increase in the strain when the humidity was increased from 0% RH to 80%RH. **Figure 3.4** shows evidences of this increment and that neat PPTA fibers were more affected by fatigue than those that were sonicated. Although sonicated fibers appeared to experience less creep, they were still affected by humidity. These results indicate the important role of humidity on PPTA fibers.
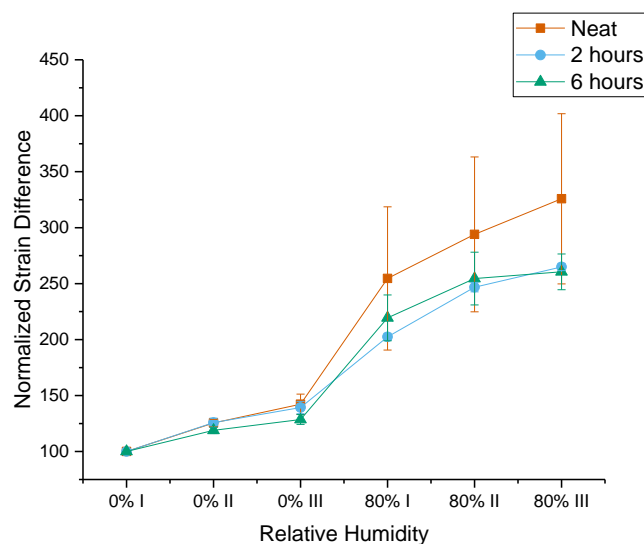
Figure 3.4 Results of the cycle-humidity DMA test. Normalized.

Long creep test

In contrast with the last experiments, the long creep test was made to detect how important the role of water is on the fibers and if hydrogen bond formation is occurring. In this test, fibers were sonicated in water and in hexane for two hours. It was expected that hexane would not cause formation of hydrogen bonds or layers between the PPTA crystallites. Therefore, samples sonicated under these conditions showed the direct effects of sonication.
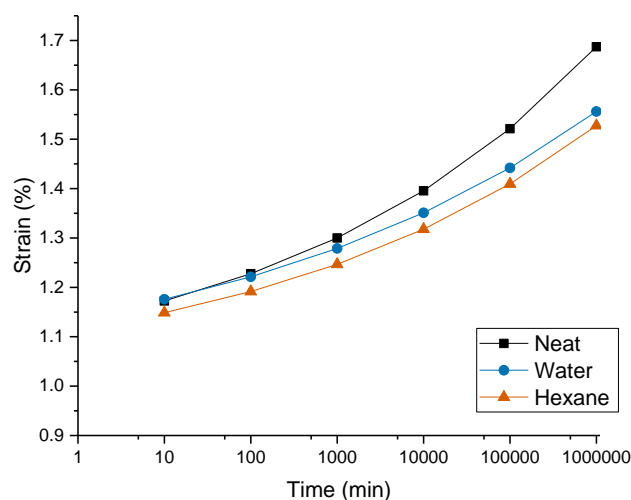
Figure 3.5 *Long term predictions based on the DMA long creep test on fibers sonicated for two hours in water and hexane.*

Figure 3.5 shows that neat fibers experienced more creep than fibers sonicated for two hours in both water and hexane. On the other hand, hexane displayed the lowest amount of creep. Comparing results on the neat and sonicated fibers in hexane demonstrates the positive effects of sonication. Since hexane is not a good solvent for PPTA fibers, it was determined that the reduction in creep was due to changes in the physical structure of the fibers caused by sonication. This indicates that sonication hinders the creep response on the fibers. However, fibers sonicated in water showed more creep than those in hexane. This is related to the formation of layers of water between the PPTA crystallites. Overall, sonication does hinder the creep effect on fibers, but the presence of water counteracts this effect, increasing the amount of creep.

Results of these three DMA experiments confirm the formation of water layers between PPTA crystallites proposed by Wang et al. that was previously discussed. A single layer reinforces the strength of the bonds between the crystallites. However, when more water is introduced, more

layers are formed, and the strain increases as seen in **figure 3.4**, which indicates more chain movement.

3.4.4 Tensile testing

Tensile testing to failure was carried out to verify the influence of humidity on neat and sonicated PPTA fibers on their mechanical properties. For each condition (neat, 2 hours, and 6 hours sonication in water), an additional condition was applied in which the fibers were exposed to 50%RH for 24 hours at 30ºC. The two parameters on which this research focused on these experiments are the modulus and the peak load at failure. Twaron fibers, like the ones acquired, have a theoretical modulus ranging from 60 to 120 GPa. Neat fibers showed a decrease in modulus after 24 hours of exposure to 50% relative humidity. Furthermore, the modulus decreased after sonication. Fibers sonicated for 2 hours were less affected by humidity. On the other hand, fibers sonicated for 6 hours had a slight increase in the modulus but was later decreased after exposure to humidity. However, no great changes in the elastic modulus was detected among the sonicated fibers (**figure 3.6**) and they were all within the range of the theoretical values of PPTA fibers. Overall, the presence of water after 24 hours had a major effect on the modulus of the fibers.
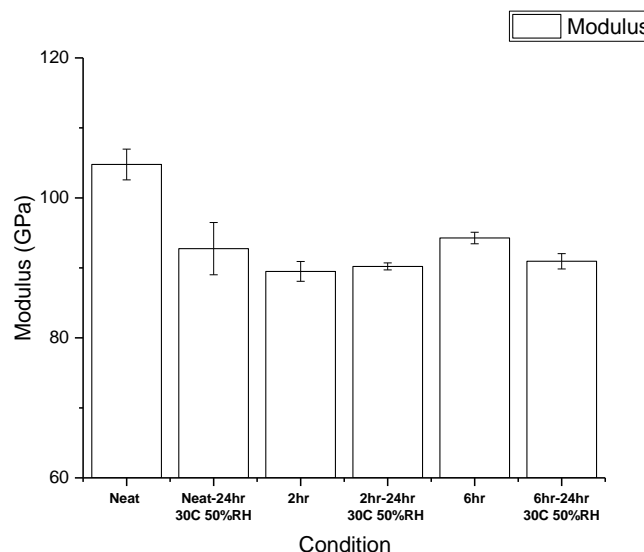
Figure 3.6 *Elastic modulus of neat and sonicated fibers after sonication and 24 hours in the humidity chamber at 30oC and 50% RH.*

More relevant information is obtained when the peak load is analyzed. Results are demonstrated in **figure 3.7** and reveal that sonicated fibers have a higher stress at failure when compared to neat fibers. Neat fibers did not show any significant difference in the stress after 24 hours of 50%RH at 30°C. Overall, stress increased with sonication time. However, after being exposed to humidity for 24 hours, the higher peak load previously achieved through sonication was decreased. This effect is more notable on fibers sonicated for 6 hours, although, fibers that were sonicated for 2 hours had a slight decrease. Nevertheless, neat PPTA fibers showed a lower peak load compared to their sonicated counterparts. A more drastic change was seen on fibers sonicated for 6 hours, for which humidity severely decreased the peak load. This indicates that humidity played an important role in creep and failure of PPTA fibers.

Thus, results from this test revealed that sonication affects the structure of the fibers and their mechanical properties like the elastic modulus and ultimate tensile stress. These mechanical properties are attributed to the pleated structure and crystalline organization of the molecules[66].
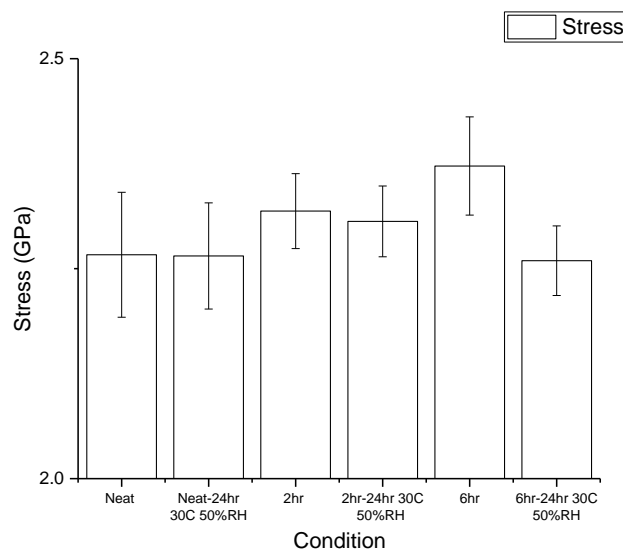
Figure 3.7 *Peak load of neat and sonicated fibers after sonication and 24 hours in the humidity chamber at 30oC and 50% RH.*

3.4.5   PALS
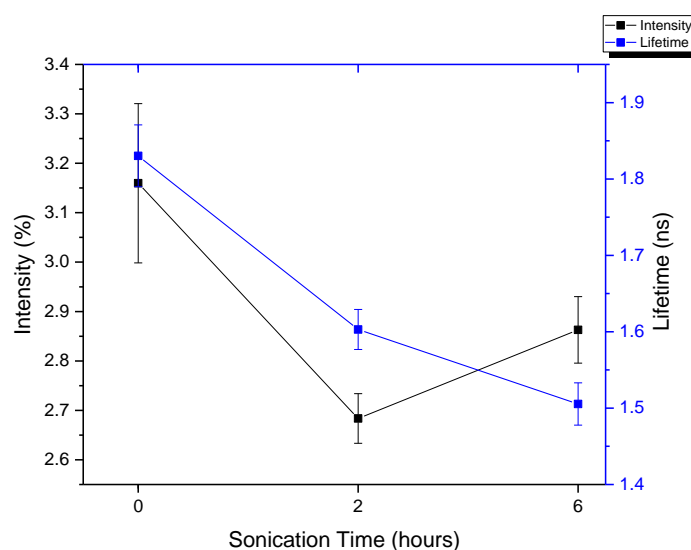
Figure 3.8 *PALS lifetime and intensity data as sonication takes place.*

According to PALS data, the lifetime of the positron was reduced significantly when compared to neat fibers, which indicates that the size of the free volume is reduced (**figure 3.8**). Therefore, tensile strength might be increased as sonication time increases due to the reduction of the space between the molecules or a re-arrangement of the crystalline domains in the fibrillar structure of the fibers. On the other hand, the intensity of the lifetime indicated the quantity of the free volume of that size in the material. **Figure 3.8** also shows that the intensity decreased as sonication occurred, but after 6 hours it slightly increased, which means that more free volume areas are created.

To understand the overall effect of sonication on the fibers, the fractional free volume is calculated using **equation 2**. This equations is the product of the intensity and the free volume areas where the annihilation occurs, assuming they are spherical ($V_f = \frac{4}{3}\pi R^3$)[46].

$$Fractional\ V_f = I_{oPs} \times \frac{4}{3}\pi R^3$$

Equation 2. Calculation of the fractional free volume of a material. The value of R is taken from results of the Tao-Eldrup Equation.

These calculations demonstrate that the free volume did decrease with sonication (**figure 3.9**). What was obtained from these results can mean one of three things: (a) there is a real reduction of the free volume, (b) there is water trapped in the free volume after drying, or (c) both events are taking place. A reduction of the fractional free volume can be seen when water occupies the voids in a material since the positrons do not distinguish between the water electrons and those from the fibers. Therefore, the increase in tensile strength (stress at fracture) seen in **figure 3.7** can be caused by a combination of the re-arrangement of the crystalline structure of the fibers and the presence of a water monolayer.
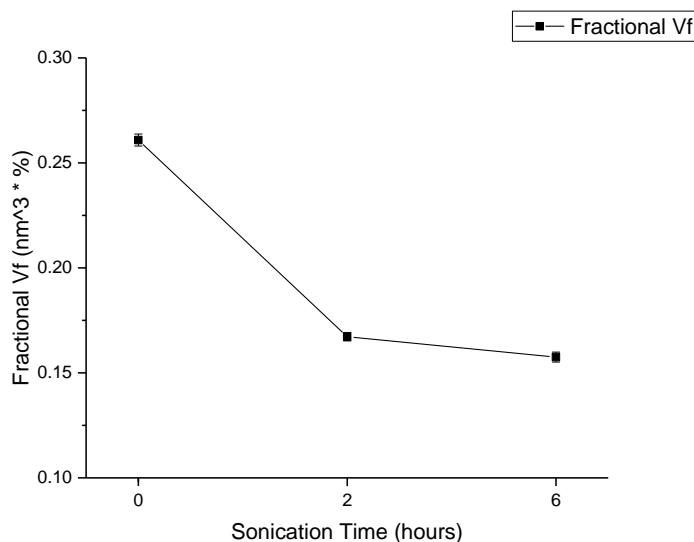
Figure 3.9 *PALS data shows that free volume decreases in PPTA fibers as sonication takes place.*

3.4.6   Small Angle X-Ray Scattering (SAXS)

Complementary data to PALS was acquired using SAXS. The data shown in **figure 3.10** is normalized by transmittance. Reflections indicate two different domain spacings (q_1* = 14.6 nm^{-1} d = 0.43 nm; q_2* = 16.3 nm^{-1}, d = 0.37 nm) that are close in size and both exhibit a high degree orientation, as is evident from multiple strong reflections at higher q values. The secondary reflections for q_2* are obscured by the stronger reflections of q_1* in the smoothed curves in **figure 10**. From literature, this scattering is attributed to the crystalline domains of the fiber core[67]. As postulated in the evaluation of PALS data, a layer of water molecules could remain bound to the crystallites. In this case the two reflections may be interpreted as the spacing between crystallites (q_1*) and the spacing between water layers of adjacent crystallites (q_2*). No shift in the primary reflection is observed with sonication, indicating that the spacing of crystalline domains is not altered.
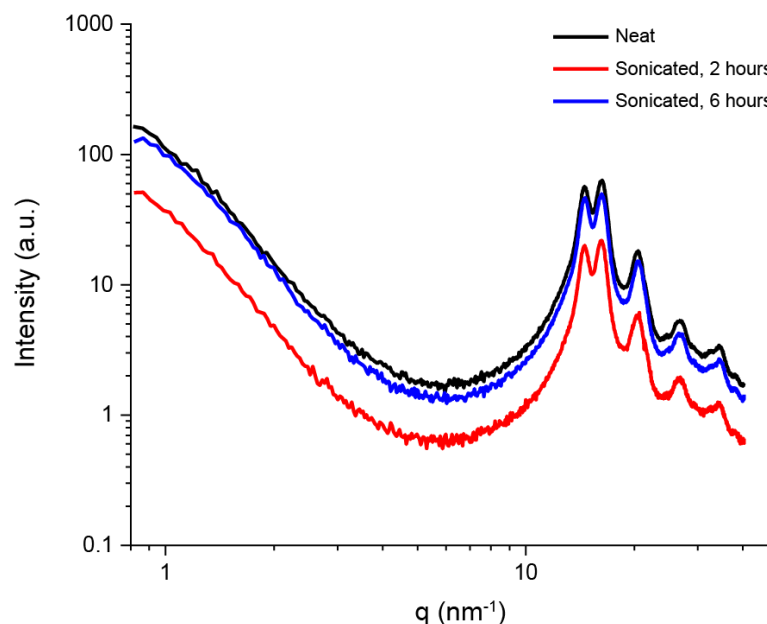
Figure 3.10 *SAXS data of neat and sonicated PPTA fibers.*

Scattering profiles were normalized by transmittance in order to gauge the relative intensity of scattering from the neat, 2 hours, and 6 hours samples. The scattering intensity can be directly correlated to the degree of alignment between crystalline domains. The decrease in intensity at 2 hours of sonication suggests a decrease in alignment of crystalline regions. Although the intensity at 6 hours of sonication remains lower than that of neat fibers, it is higher than the signal for the 2-hour sample, suggesting the crystallites are better aligned after 6 hours than after 2. This effect has been seen in literature as a function of strain, where authors saw a decrease in crystalline alignment at low strains and partial realignment at higher strains[67]. Note that realignment of crystalline domains at this length scale does not necessarily mean there was no increase in degradation of the fibrils at larger length scales and is therefore not in conflict with mechanical testing results.

3.5   **Conclusions**

Small changes in the mechanical properties such as the creep response of PPTA fibers can be detected through dynamic mechanical analysis. Said technique allows the instant measurement of the changes in strain of the fibers under different percentages of relative humidity. This is a great advantage for understanding the effect of water on hygroscopic materials such as PPTA fibers.

Considering the results of the experiments carried out using this technique, PPTA fibers exhibit greater moisture uptake at lower temperatures (30°C, which is closer to room temperature) than at higher (60°C). The former case shows a higher degree of creep than the latter. The same behavior was seen for all fibers on every case -neat and sonicated-.

Sonication plays an important role in the fatigue of PPTA fibers. When compared to the neat fibers, sonicated fibers for 2 and 6 hours showed a higher resistance to creep after various creep cycles. Sonication affects the physical structure of the fibers. Results reveal that sonicating PPTA fibers for 2 hours can slightly improve their tensile strength and reduce the creep behavior at a wide humidity range and temperatures. However, excess of sonication makes PPTA fibers prone to retain more water, leading to a drastic decrease of their mechanical properties when they are exposed to humidity for long periods of time. The longer the exposure to humidity, the more formation of water layers. Overall, sonication increases the water sorption of PPTA fibers. PALS data indicates that sonication reduces the free volume in PPTA fibers, when compared to neat as-received fibers. The reduction of the free volume indicates changes in the fiber structure and the possible presence of water trapped in the free volume spaces. SAXS data supports the possibility of water trapped in these spaces.

Thus, sonication at a certain extent can enhance the mechanical properties of PPTA fibers although the presence of water decreases the achieved improvements obtained with this method.

CHAPTER 4   WATER, PH, AND SWEAT DEGRADATION

Content of this chapter is retrieved from the submitted paper "Free Volume- Performance Relationship of PPTA Fibers: Accelerated Degradation in Acid, Basic, and Neutral Aqueous Solutions". SAXS data on this paper was in collaboration with Jessica Sargent.

4.1   Introduction

Poly (p-phenylene terephthalate) (PPTA) fibers are commonly used in soft body armors due to their excellent mechanical and chemical properties. Although these fibers show great strength, high modulus and chemical resistance, they can be exposed to different factors that can decrease their performance. In this paper we will discuss the effects of DI water, acid and basic aqueous solutions (pH 4 and pH 10 respectively) and sweat. The effects of these conditions were monitored for 10 weeks. The mechanical performance of PPTA fiber was compared to changes in the nanostructure of the fibers, by measuring their free volume using a characterization technique known as positron annihilation lifetime spectroscopy (PALS).

PALS in combination with other characterization techniques such as small angle X-ray scattering (SAXS) and tensile testing are effective to measure small changes on the nanostructure of PPTA fibers at early stages of degradation. PALS revealed that PPTA fibers are able to retain more acid solutions like sweat, which alters the alignment of the crystalline domains and decreases the mechanical performance.

4.2   Background

Although PPTA fibers possess outstanding chemical and mechanical properties, their performance can be reduced overtime due to different factors in the environment and fatigue due to constant use[68][69]. PPTA fibers are mostly affected by strong acids and bases, especially at

high temperatures. Exposure to acids result in hydrolysis (chain scission) and a decrease in the mechanical performance of the fibers[30].

Interaction with a highly acid or basic chemicals is very rare during the use of bulletproof vests. A more realistic interaction with an acid would be with human sweat[70]. The combination of sweat and storage temperature may accelerate the degradation process of PPTA fibers, resulting in a decrease in their mechanical performance. The goal of this research is to detect early stages of the degradation process in acid and basic aqueous solutions, as well as in water and sweat.

Degradation is commonly detected through mechanical testing and microscopy. Significant loss of performance that is detected through these methods is the result of the sum of smaller changes in the chemical and physical structure of the fibers overtime. Therefore, early stages of degradation may not show great visual signs or loss of mechanical performance. In this study we propose detecting these small changes by measuring the dimensions of nanostructures of PPTA fibers as they degrade.

As mentioned in chapter 1, PPTA fibers have 3% to 5% by weight water, where 6% of that water is loosely bonded and 33% is tightly bonded to the crystalline domains in the fibers[15]. Therefore, interaction with water, like in cellulose nanofibrils where the radius of the free volume is reduced due to the strong interaction between cellulose and water, are crucial to understand the changes in free volume in PPTA fibers.

Accelerated degradation is commonly performed at extreme temperatures, higher than 100°C. According to A. Abu Obaid et al. these extreme temperatures may cause degradation mechanisms that are not representative of what happens under real use conditions[71]. Therefore, they performed accelerated degradation at near ambient temperatures ($\leq 100^{\circ}$C). In their study, they concluded that at temperatures above 75°C water can enter fiber's highly oriented core, which

enables the mobility of polymer chains. The latter can also cause changes in the crystal orientation and their size[71]. Diffusion of water to the core is also attributed to the mobility of the phenylenediamine rings at temperatures above 75°C [71][72][73][74].

Overall, the goal of this research is to use PALS to detect early stages of degradation on PPTA fibers that have been degraded in DI water, acid and basic aqueous solutions, and sweat.

4.3   **Experimental**

4.3.1 *Accelerated Degradation of Fibers*

Two different methods of accelerated degradation were performed on PPTA fibers: degradation in aqueous solutions with different pH and in artificial sweat. In both cases, woven PPTA material was submerged in the different solutions in closed jars covered in aluminum foil. Samples were pat dried (to remove excess water from the surface) and then oven dried at 100°C for an hour before any mechanical, PALS and SAXS testing.

a. Aqueous solutions with different pH

PPTA woven material was submerged in DI water and aqueous solutions of pH 4 and pH 10 (made with HCl and NaOH respectively). The total time of aging was 10 weeks (70 days) at 80°C. pH was monitored every week.

b. Artificial Sweat

To replicate degradation under real conditions, PPTA fibers were submerged in artificial sweat. Solutions of artificial sweat were prepared following the ISO 3160-2 standard. Sweat solutions had a pH 4.7. Aging was performed at 25°C, 50°C and 100°C for 10 weeks. Samples were tested at 2, 6, and 10 weeks of aging.

4.3.2   Characterization

To have visual evidence of degradation on PPTA fibers, images were acquired through scanning electron microscopy (SEM). Samples were sputter coated for 1 minute. Tensile testing was performed on yarn extruded from the aged woven material. An MTS Insight 100kN was used to perform tensile tests on PPTA fiber yarns. The test was performed with a 1000N load cell and fiber grip. Equipment used was a TA Instruments Q800 DMA with a tensile film fixture. A controlled force test was conducted on single fibers for neat fibers and fibers after 10 weeks of exposure. Single fibers were mounted on an index card with epoxy glue (see **figure 4.1** for reference), following the ASTM C1557 standard. This technique helps fix the fiber and its gauge length (1cm). The test consisted on a force ramp to 18 N at a rate of 0.1 N/min. Preload force was 0.001N. Around 12 samples were tested for each condition.
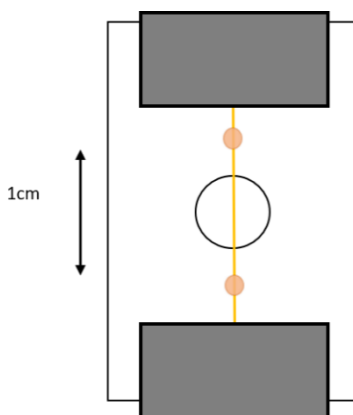
Figure 4.1 *Sketch of the setup for single fiber testing. Fiber were extracted from yarns and fixed with epoxy.*

Three experiment were carried using PALS: (1) drying, (2) degradation in aqueous solutions with different pH and DI water, and (3) sweat degradation. For the drying experiment, the free volume of a sample of neat woven PPTA fibers was measured with PALS. After data was collected, the sample was submerged in water for 48 hours and measure with PALS. Once data of

the wet sample was collected, the sample was dried at 80ºC for 4 hours and PALS measurement were collected. The same procedure was performed when the sample was dried further at 100ºC for 2 hours. The purpose of this experiment was to understand how water affects the free volume.

Folded woven PPTA material was used for PALS experiments. PALS experiments were performed at room temperature. A Na^{22} source was used for these tests. Each test consists of a million counts or more -approximately 3 days- to have a better fit. Fitting of the curves was done using a software called PALSfit. The fit considered 3 lifetimes. Details of the SAXS experiments are the same as in chapter 3.

4.4   **Results and Analysis**

4.4.1   *pH Monitoring*

Fibers at pH 4 (**figure 4.2**) showed a greater change of pH a after a week at 80ºC than fibers at pH 10 (**figure 4.3**). For fibers degraded in pH 4 solutions, the value of the pH increased from 4 to 9 after one week at 80ºC. As degradation takes places, the pH decreased with time. This indicates that a chemical reaction like hydrolysis took place. On the other hand, pH 10 samples have a slight decrease in pH after a week at 80ºC. Moreover, the great difference after each week for fibers at pH 4 indicates a greater degradation rate than fibers in DI water and pH 10 solutions.

Previous studies by Arrieta et al., show that hydrolysis takes place in Kevlar fibers when exposed to water at high temperature and, as a result of chain scission, carboxylic acid and an amine group are formed [30]. Traces of sulfuric acid can be found in Kevlar fibers after the spinning process. Therefore, water acts as a catalyst for the hydrolysis reaction in the fibers. A similar process is happened for fibers in pH 4 solutions. The formation of amine groups as a result of the hydrolytic reaction, neutralize the solution. Nevertheless, as more acid is added every week, the concentration of H_3O^+ increased consequently reducing the pH.
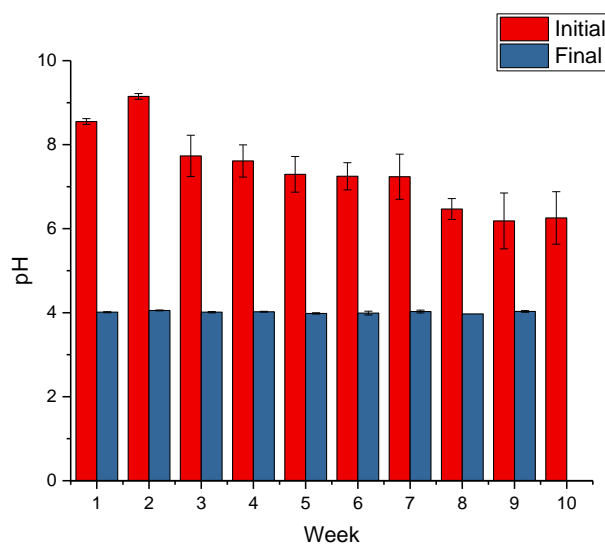
Figure 4.2 *Monitoring of the pH 4 the aqueous solutions used to degrade PPTA fibers at 80ºC. Final values indicate the pH after it was adjusted for further degradation.*
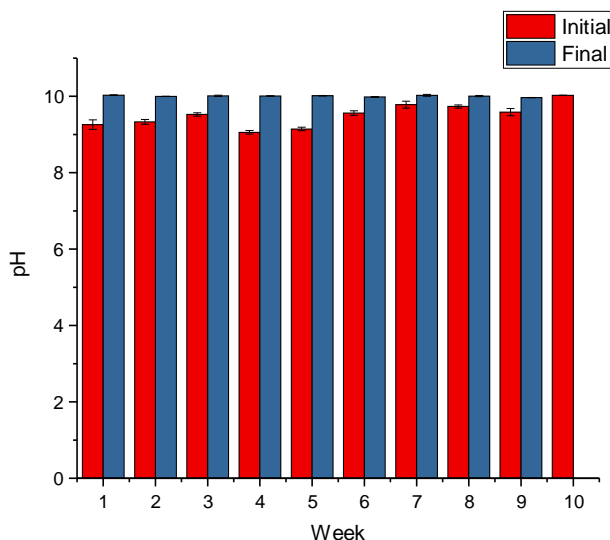
Figure 4.3 *Monitoring of the pH 10 the aqueous solutions used to degrade PPTA fibers at 80ºC. Final values indicate the pH after it was adjusted for further degradation.*

NaOH was used to make pH 10 aqueous solutions. It is known that NaOH is used to neutralize the fibers after being submerged in H_2SO_4 in the production process. As a result of that neutralization, $NaSO_4$ is obtained. The latter is the principal impurity found in PPTA fibers[75]. $NaSO_4$ is slightly more alkaline. The neutralization of traces of H_2SO_4 may explain the decrease in the pH 10 solutions to around pH 9 (as seen on **figure 4.3)**. This is a small change when compared to the results of fiber in pH 4.

4.4.2   SEM Images

SEM images show that there is little to no degradation for fibers submerged in DI water and pH 10 solution (**figure 4.4 to 4.12**). On the other hand, pH 4 at 10 weeks shows degradation at the fibers surface. Overall, fibers in pH 4 solution are degraded at a higher rate than fibers degraded at pH 10 and DI water. This visual evidence supports that fibers degrading in pH 4 solutions degrade at a higher rate due to of hydrolysis.

HCl has greater interaction with the PPTA molecules, as noted by their lower volume when compared to fibers in the other conditions. Temperature and the presence of an acid accelerate the hydrolysis reaction of PPTA chains, leading to loss of mechanical performance. Fibers degraded in sweat showed no visual signs of degradation.
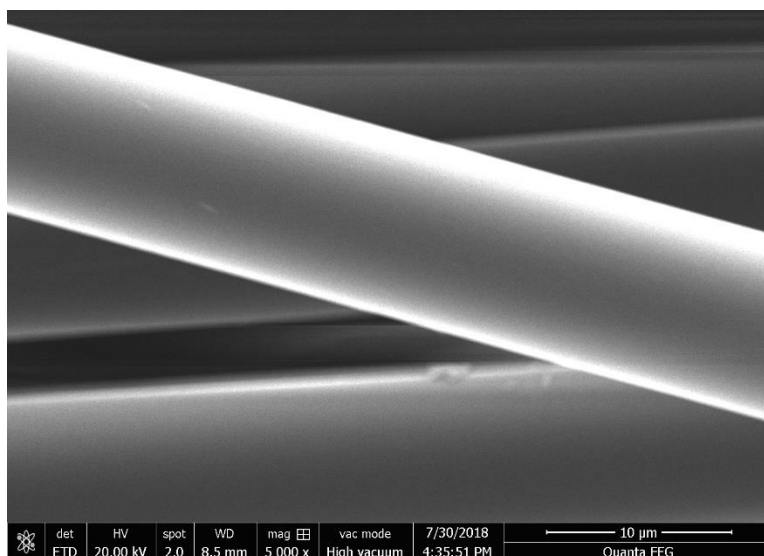
Figure 4.4 *PPTA fibers degraded in DI water for 2 weeks.*
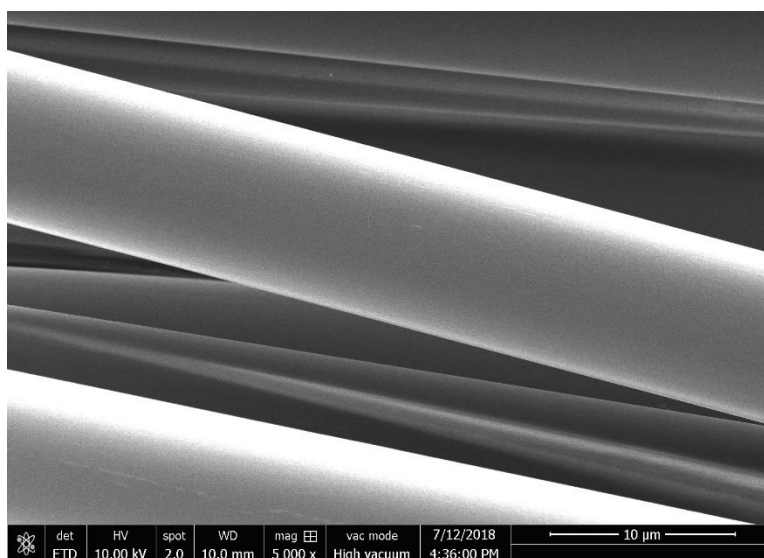
Figure 4.5 *PPTA fibers degraded in DI water for 6 weeks.*
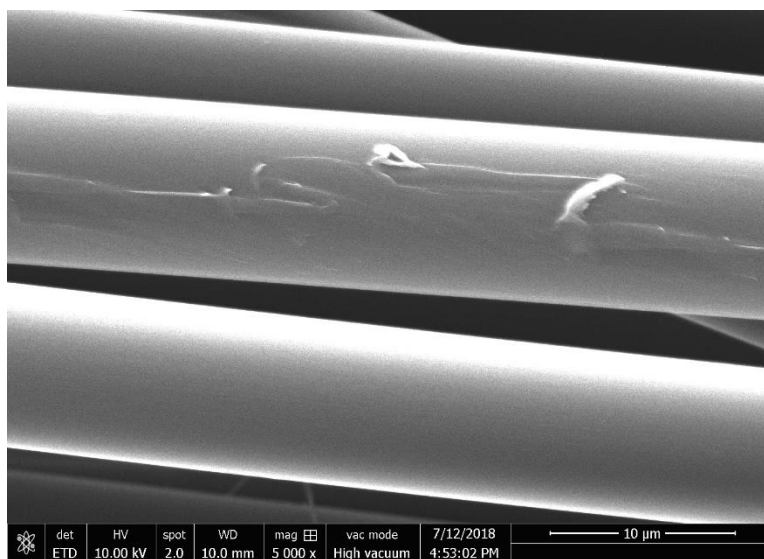
Figure 4.6 *PPTA fibers degraded in DI water for 10 weeks.*
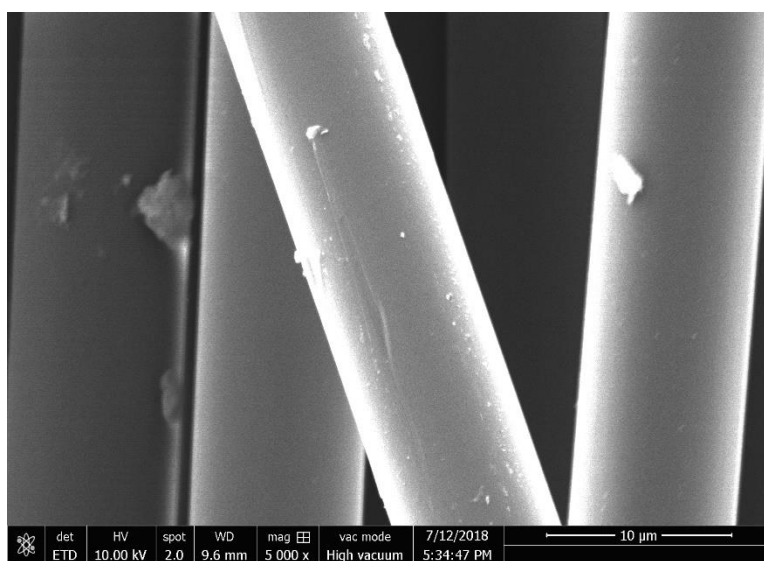
Figure 4.7 *PPTA fibers degraded in pH 4 aqueous solutions for 2 weeks.*
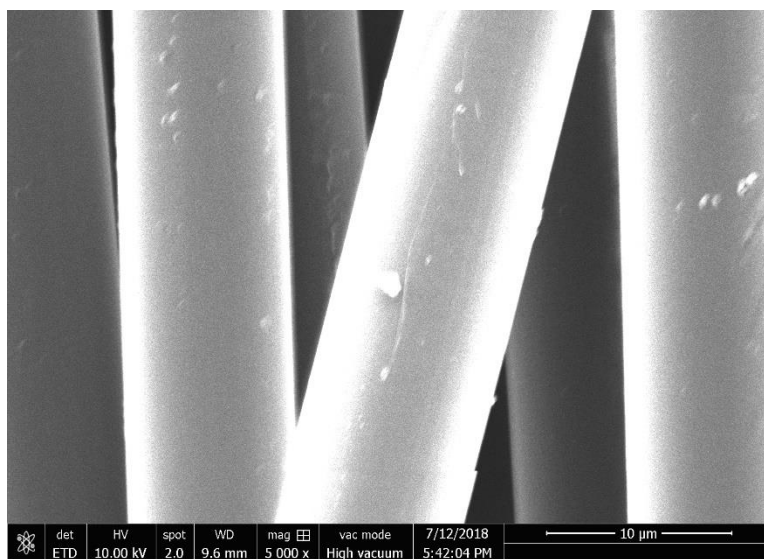
Figure 4.8 PPTA fibers degraded in pH 4 aqueous solutions for 6 weeks.
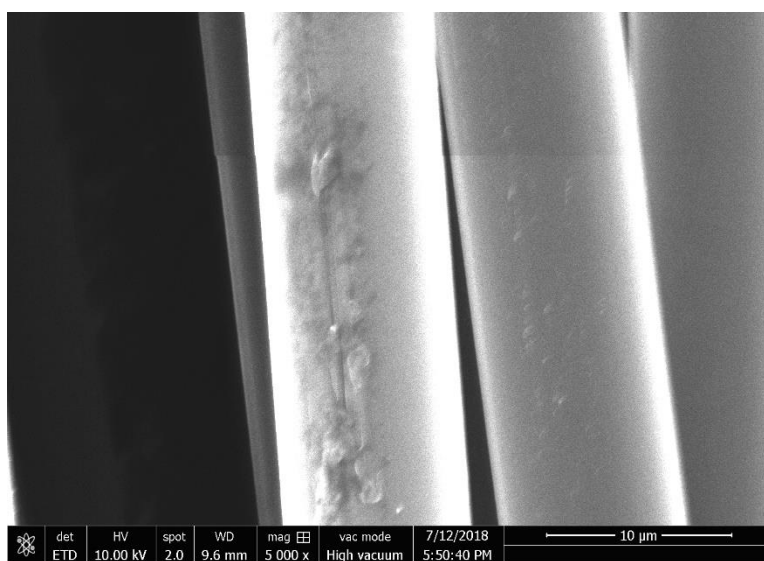
Figure 4.9 PPTA fibers degraded in pH 4 aqueous solutions for 10 weeks.
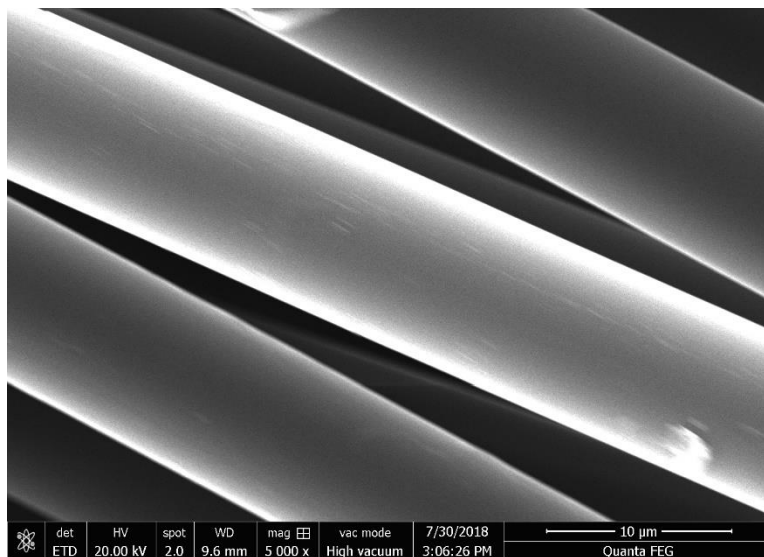
Figure 4.10 PPTA *fibers degraded in pH 10 aqueous solutions for 2 weeks.*
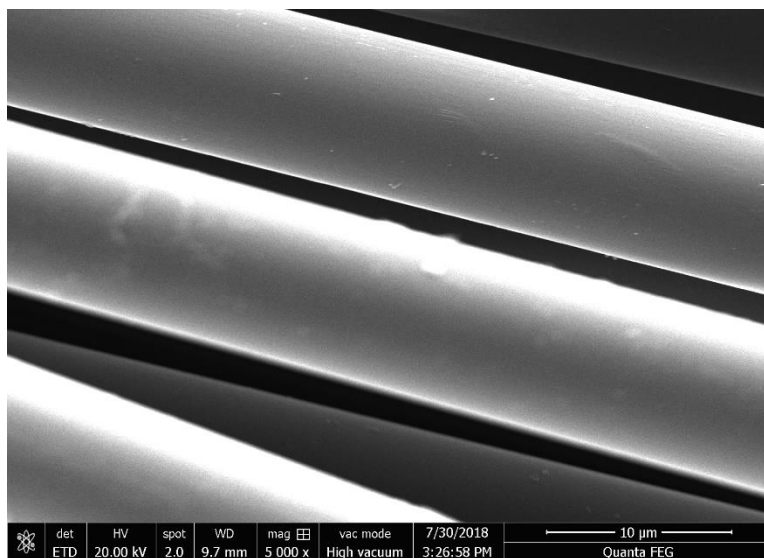
Figure 4.11 PPTA *fibers degraded in pH 10 aqueous solutions for 6 weeks.*
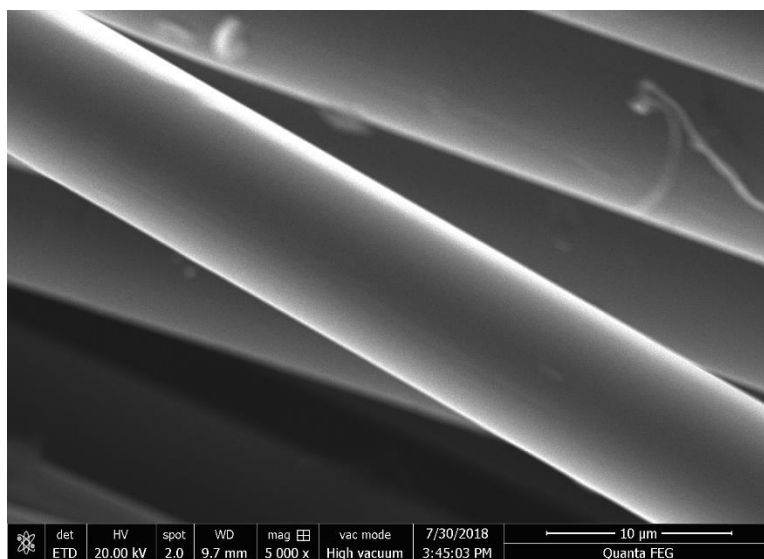
Figure 4.12 *PPTA fibers degraded in pH 10 aqueous solutions for 10 weeks.*

4.4.3   Tensile testing

There were no great changes in the modulus for the fibers within each condition (**figure 4.13**). The formation of defects in the fiber structures did not affect the modulus. This is because the modulus is a global parameter of the orientation and alignment of the crystallites in the fiber[76]. However, the ultimate tensile strength of the degraded fibers showed more clear changes. The ultimate tensile strength is affected by the formation and accumulation of defects as well as differences in the crystallite orientation between the skin and the core of the fibers[76][77]. Other than the formation of defects, the accumulation of water also alters the strength of PPTA fibers. Water can interact with PPTA fibers by intercalating between the crystalline domains[17]. Water layers are formed over time between the crystalline domains. At low relative humidity monolayers of water are formed. These monolayers have a stronger bond with the crystallites and higher creep activation energy compared to the activation energy of water multilayers formed at higher relative humidity[18]. The effects of water and interactions with HCl and NaOH were considered to analyze the mechanical performance of the PPTA fibers.

For the purpose of showing a clearer trend of the phenomena, only data for 2 and 10 weeks is shown. As mentioned before, the modulus of the degraded fibers did not change significantly with respect of the neat fibers. However, changes were detected on their strength (**figure 4.14**). After two weeks of degradation, the strength of fibers degraded in all conditions was close to the strength of neat fibers. After ten weeks of degradation, fibers submerged in pH 4 solutions had a clear decrease on their strength. On the other hand, fibers in DI water had an increase in their strength. This effect can be related to the intercalation of water and the formation of water monolayers in between the crystallites, which slightly increase the strength due to the formation of hydrogen bonds. Fibers degraded in pH 10, show no great change in the strength. Overall, we can conclude that fibers degraded in pH 4 had a faster, greater and more noticeable decrease in their strength. This result, along with those found from monitoring the pH values, are evidence of degradation through hydrolysis. A t-test was performed on the values obtained through this test and it is discussed in the appendix of this thesis.

Mechanical performance of fibers degraded in pH 10 solutions showed no considerable decrease. These results go along with the results obtained from the pH monitoring, where there was no great change.
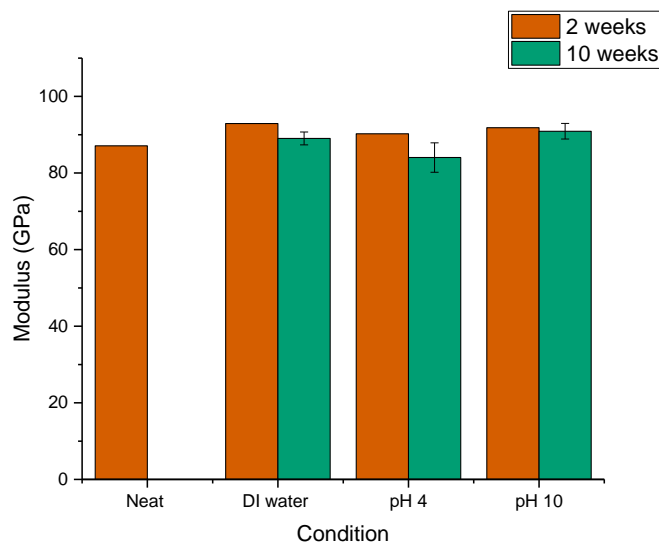
Figure 4.13 *Results of the tensile tests on PPTA yarns degraded in different pH - modulus*
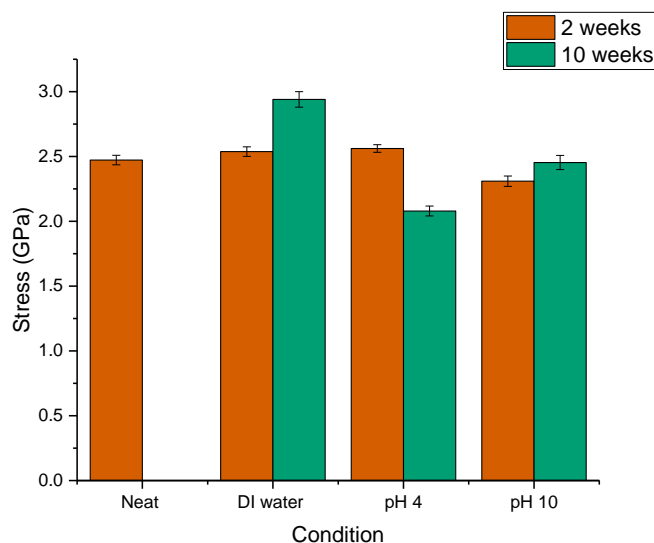
Figure 4.14 *Results of the tensile tests on PPTA yarns degraded in different pH - ultimate tensile strength.*

There was no variance on the modulus of PPTA fibers degraded in sweat (**figure 4.15**). Although the sweat solutions used for this experiment had a pH 4.7, it had a greater effect on the strength of the fibers when compared to fibers degraded in pH 4 solutions (mix of HCl and water). This was due to the different acids and salt components in the sweat solution. The ultimate tensile

strength on fibers degraded in sweat solutions is less than the neat fibers and decreased slightly with time (**figure 4.16**). This decrease was sharper at 100°C and can be attributed to the effects of temperature and interactions of the different components of sweat with the PPTA molecules. A t-test was also performed on the values obtained through this test the results are discussed in the appendix.

It is known from previous studies that at temperatures higher than 75°C, more molecules can diffuse to the core of the fiber (where there are more crystalline domains), since at that temperature motion of the diamine rings on the PPTA molecules occur[71]. Hence, a greater decrease was seen for fibers degraded in sweat at 100°C.
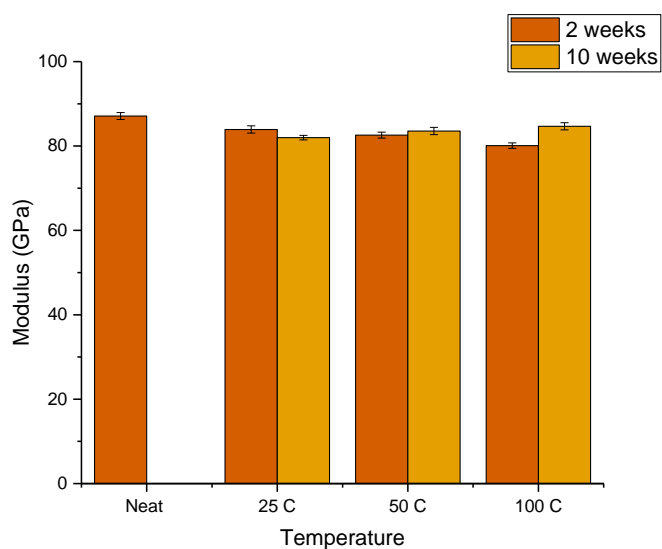
Figure 4.15 *Modulus at break of the fibers degraded in artificial sweat at different temperatures and weeks.*
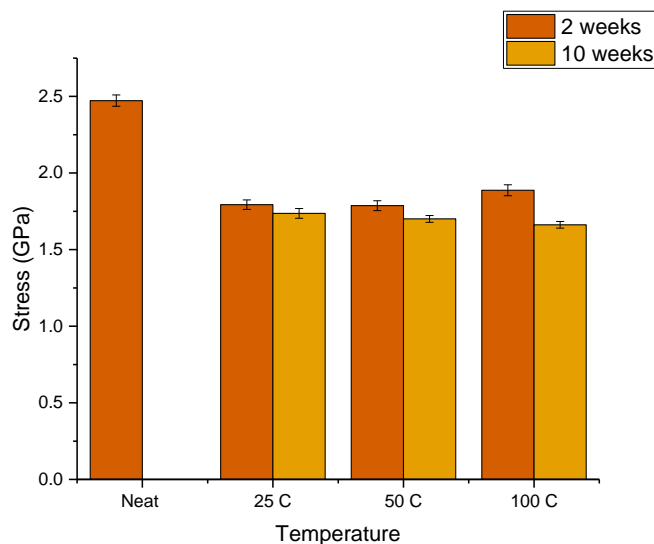
Figure 4.16 *Ultimate tensile strength of the fibers degraded in artificial sweat at different temperatures and weeks.*

4.4.4   Dynamic Mechanical Analysis

Results of DMA (**figure 4.17**) tests showed after 10 weeks no great difference is perceived in the modulus of single fibers. However, significant changes were detected on the tensile strength (**figure 4.18**). After 10 weeks of exposure, fibers at pH 4 retained only 75% of their original load. The sharper decrease in both the load and strain for fibers at pH 4, along with the results of the pH monitoring, confirms that the fibers degrade at a higher rate under acid conditions.
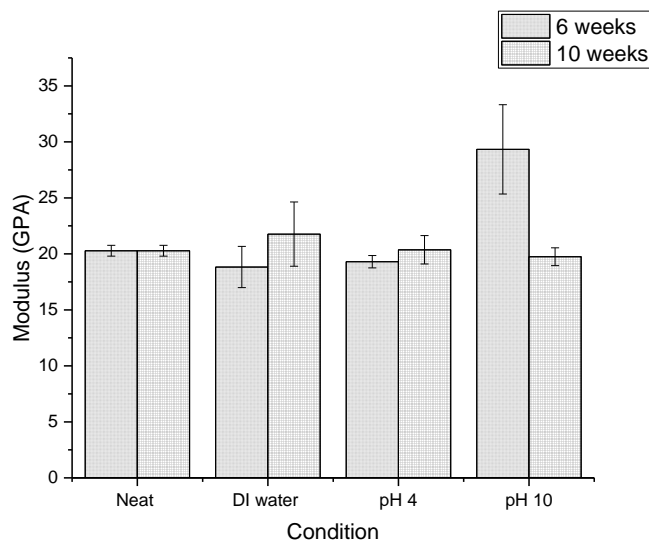
Figure 4.17 DMA results of the modulus of single fibers
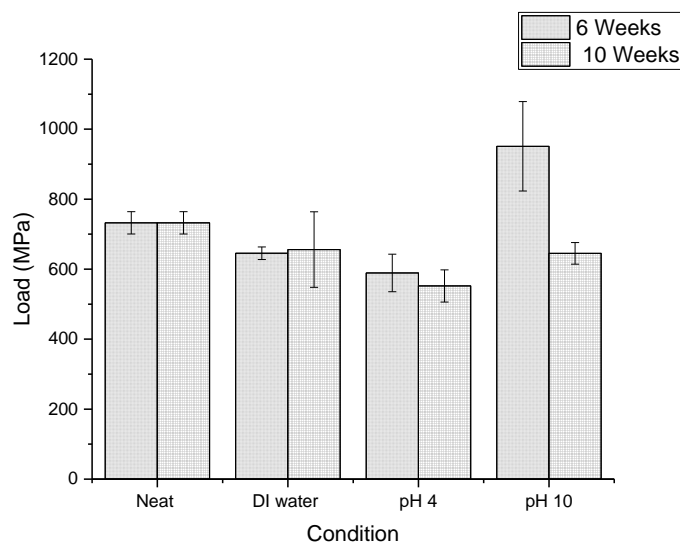
Figure 4.18 *DMA results of the ultimate tensile strength of single fibers.*

According to this data, which is similar to the results in the yarns tests (**figure 4.14**), fibers degraded at pH 10 have an increase in the modulus and the load after 6 weeks, followed by a decrease in the same mechanical properties as more degradation takes place. This might occur due to the interaction between NaOH and the impurities that might be present in the fibers. NaOH is

used to neutralize the H_2SO_4 during the spinning and production of PPTA fibers. This neutralization has a salt (Na_2SO_4) as a product, and it is removed with water[75]. Residual H_2SO_4 might still be present in the fiber causing further neutralization and an increase in the mechanical properties of the fibers at 6 weeks. Once neutralization was completed, more degradation occurred, and the performance of the fibers decreased.

4.4.5 *Positron Annihilation Lifetime Spectroscopy (PALS)*

There are two main phenomena that occur in the V_f of the fibers as they are exposed to the solvents: saturation and expansion. In terms of PALS data, saturation occurs at the time with the lowest lifetime. Expansion occurs after saturation, when the solvent molecules begin pushing the "walls" of the voids and it is indicated by an increase in the lifetime of the o-Ps.

All samples degraded under the different conditions (DI water, pH 4 and pH 10), had lower lifetime (**figure 4.19**) and V_f than the neat samples after 2 weeks two weeks of degradation. After ten weeks of degradation both the lifetime and the V_f increased. The decrease in the free volume after 2 weeks of degradation indicates that the solvent occupied the V_f areas. Data suggests that under these experimental conditions the V_f is saturated at around 2 weeks of degradation. As degradation continues V_f increases, meaning that there is an expansion. Fibers degraded in pH 4 had the greatest increase in the lifetime.

On the other hand, the intensity (which is related to the amount of free volume in the material), remained the same to the neat after 2 weeks of degradation in DI water and pH 10 (**figure 4.20**). For fibers in pH 4 the intensity decreased compared to the neat fibers. Ten weeks later, the intensity increases for all cases. Nevertheless, the intensity of fibers degraded in pH 4 remained lower that the intensity of neat fibers.

The greater decrease in intensity on fibers degraded in pH 4 solution is due to the affinity between the HCl and the PPTA molecules the electronegativity. The increase in the intensity after ten weeks is the combination of the formation of new free volume/voids and the expansion of smaller voids that were not detected before.

In all cases, the fractional free volume decreased after two weeks, compared to the neat fibers, and increased after ten weeks of exposure (**figure 4.21**). The changes on the V_f are similar on all cases.
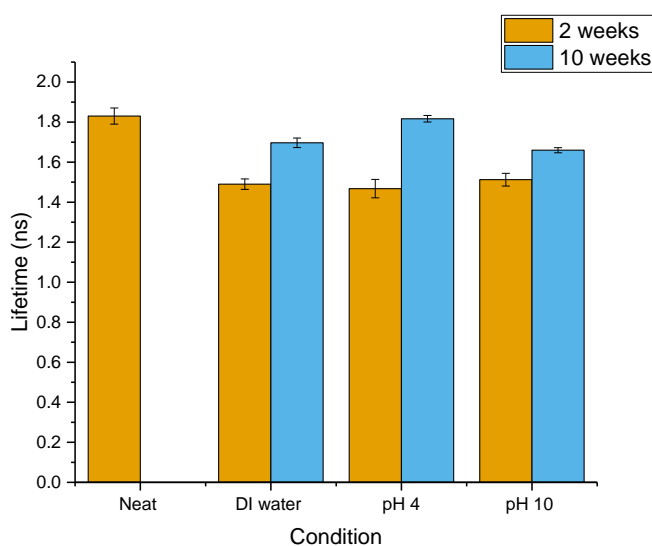
Figure 4.19 *Lifetime of fibers degraded in DI water, pH 4, and pH 10 solutions for two and 10 weeks at 80ºC.*
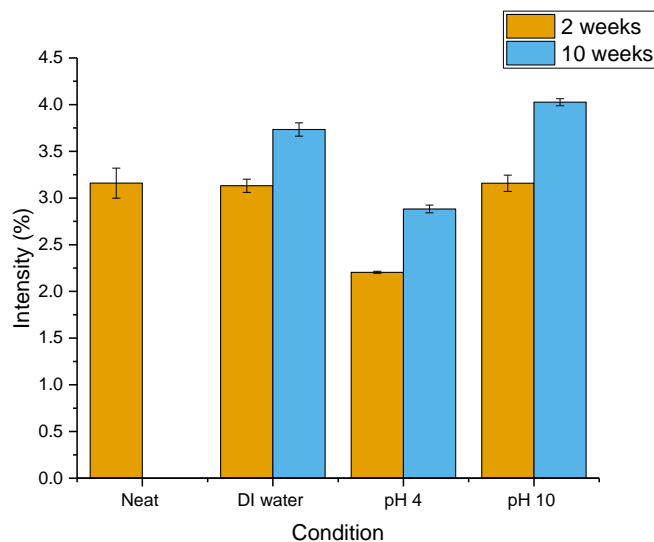
Figure 4.20 *Intensity of fibers degraded in DI water, pH 4, and pH 10 solutions for two and 10 weeks at 80ºC.*
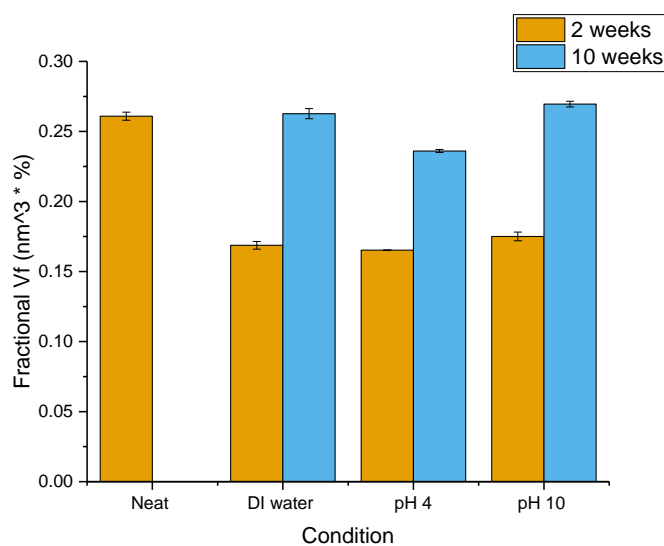
Figure 4.21 *Free volume (right) of fibers degraded in DI water, pH 4, and pH 10 solutions for two and 10 weeks at 80ºC.*

Like the experiments on aqueous solutions, the lifetime of the o-Ps decreased after 2 weeks in sweat. However, the lifetime increased with temperature (see **figure 4.22**). After ten weeks the lifetime increased for fibers at 25ºC and 50ºC, but only a small increase was seen for fibers in

sweat degraded at 100°C. This means that the expansion of the size of the free volume increases is accelerated with temperature. Data showed that the expansion reached a plateau since at 100°C there is not great change in the lifetime after 10 weeks of degradation.

On the other hand, the intensity of the o-Ps decreased with temperature and time (**figure 4.23**). At 25°C there was no great change on the intensity when compared to the neat fibers. A small increase in the intensity in this case can be attributed to expansion of small free volume areas that were not detected before. There was a clear decrease in intensity at 50°C after 2 and 10 weeks. At 100°C there is a plateau as in the lifetime.

Sweat is more effective to fill the free volume areas than simple solutions like the aqueous solutions used on the previous experiment (**figure 4.24**). This is due to the variety of components of sweat. The artificial sweat used in this experiment consists of a combination of sodium chloride, ammonium chloride, urea, acetic acid, lactic acid, and sodium hydroxide. The presence of these components and temperature contribute to a global saturation in the fibers. Hence, the intensity decreased with temperature.
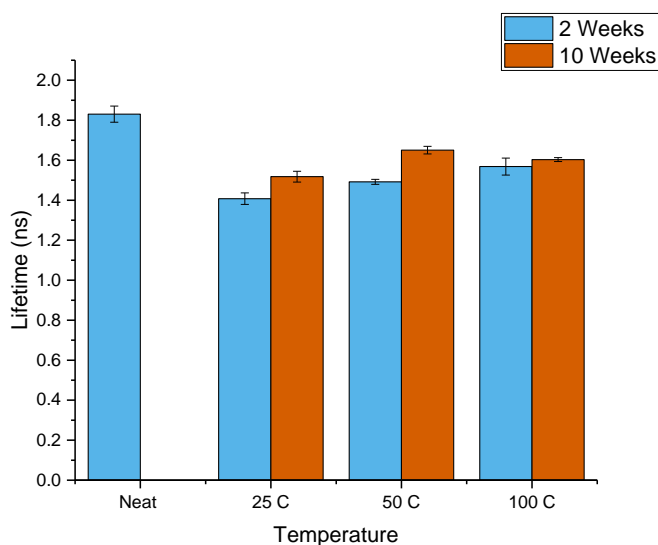
Figure 4.22 *Lifetime of fibers degraded in artificial sweat for two and ten weeks at 25°C, 50°C, and 100°C.*
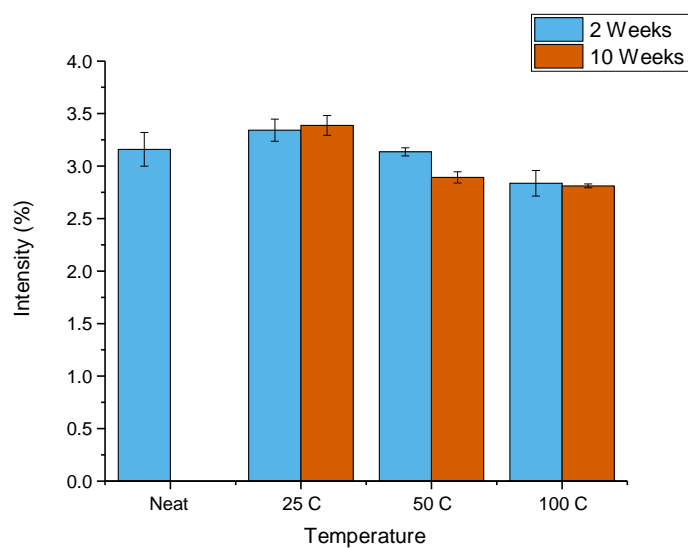
Figure 4.23 *Intensity of fibers degraded in artificial sweat for two and ten weeks at 25ºC, 50ºC, and 100ºC.*
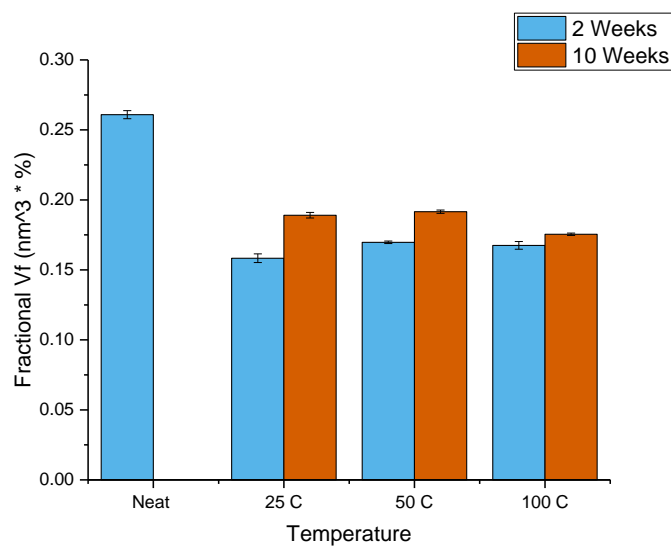
Figure 4.24 *Free volume of fibers degraded in artificial sweat for two and ten weeks at 25ºC, 50ºC, and 100ºC.*

The mechanical performance of the PPTA fibers degraded by sweat can be attribute to presence of the sweat components between the crystallites, their expansion and saturation. Both

saturation and the increase in intensity can lead to a decrease on the mechanical performance of PPTA fibers.

4.4.6 SAXS results

The intensity of the SAXS data is directly related to the alignment of the crystalline structures within the fibers. This means that the lower the intensity, the lower the alignment. **Figure 4.25** to **4.27** shows the SAXS results for the fibers degraded in DI water, pH 4, and pH 10 aqueous solutions. Like in PALS, fibers degraded at pH 4 showed the lowest intensity. Whereas fibers degraded in DI water and pH 10 showed no great difference in intensity to the neat fibers.
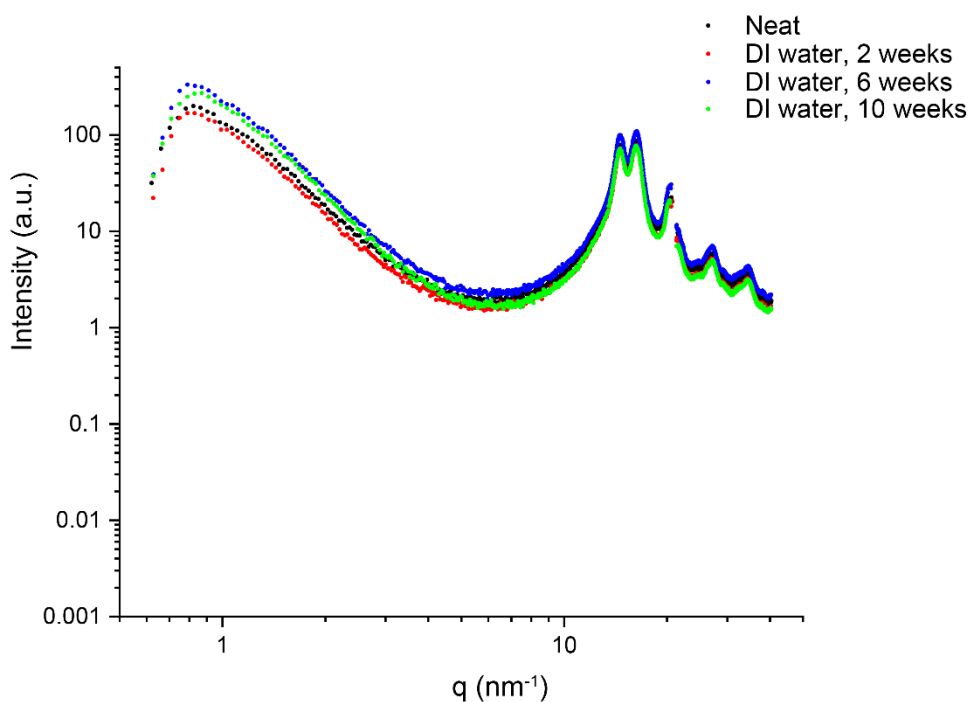
Figure 4.25 SAXS data of PPTA fibers degraded in DI water.
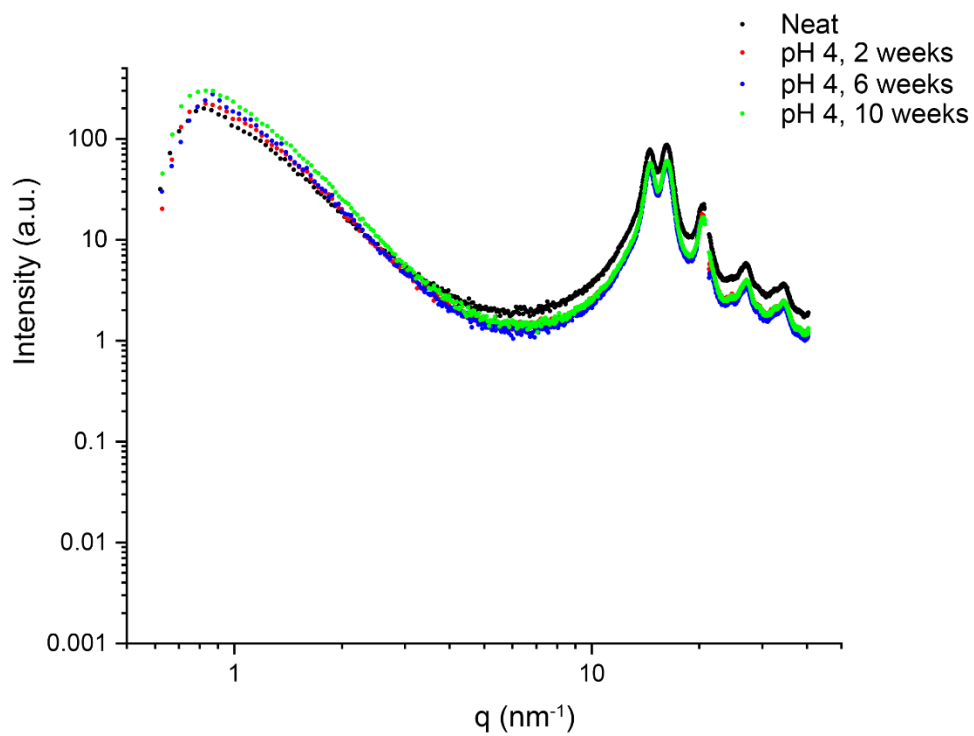
Figure 4.26 SAXS data of PPTA fibers degraded in pH 4 aqueous solutions.
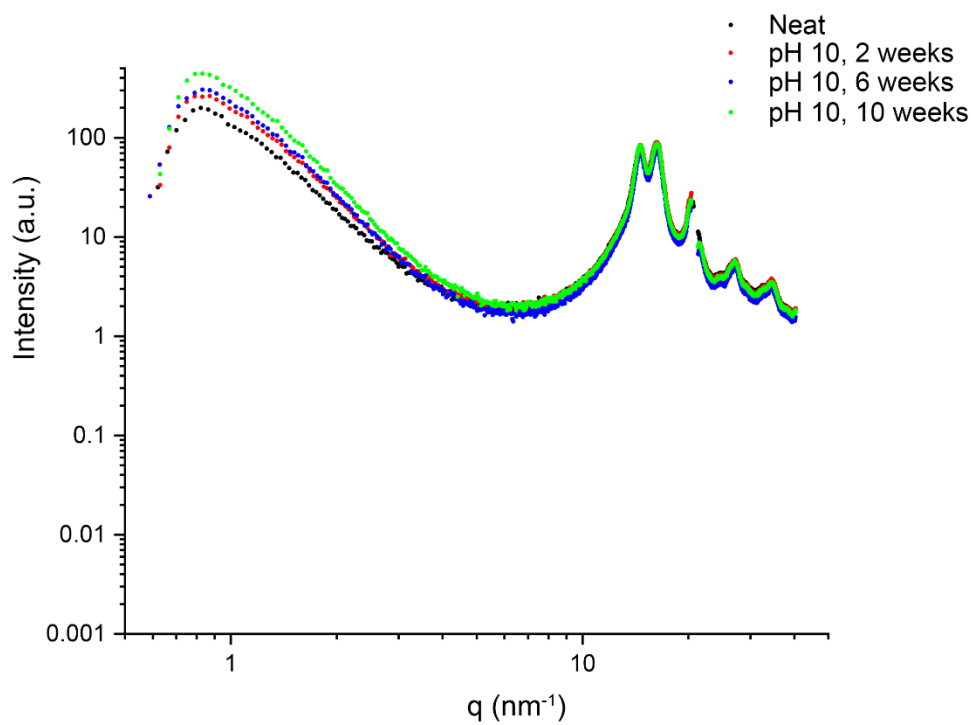
Figure 4.27 SAXS data of PPTA fibers degraded in pH 10 aqueous solutions.

On the other hand, **figure 4.28** to **4.30** shows the SAXS results for sweat degraded fiber at different temperatures. At 25 ^{O}C, the intensity slightly decreases with time. However, for 50ºC and 100ºC there was clear difference between the intensity of the neat fibers and the degraded. This, along with the result form PALS, shows that more disruption occurs with time and higher temperatures.
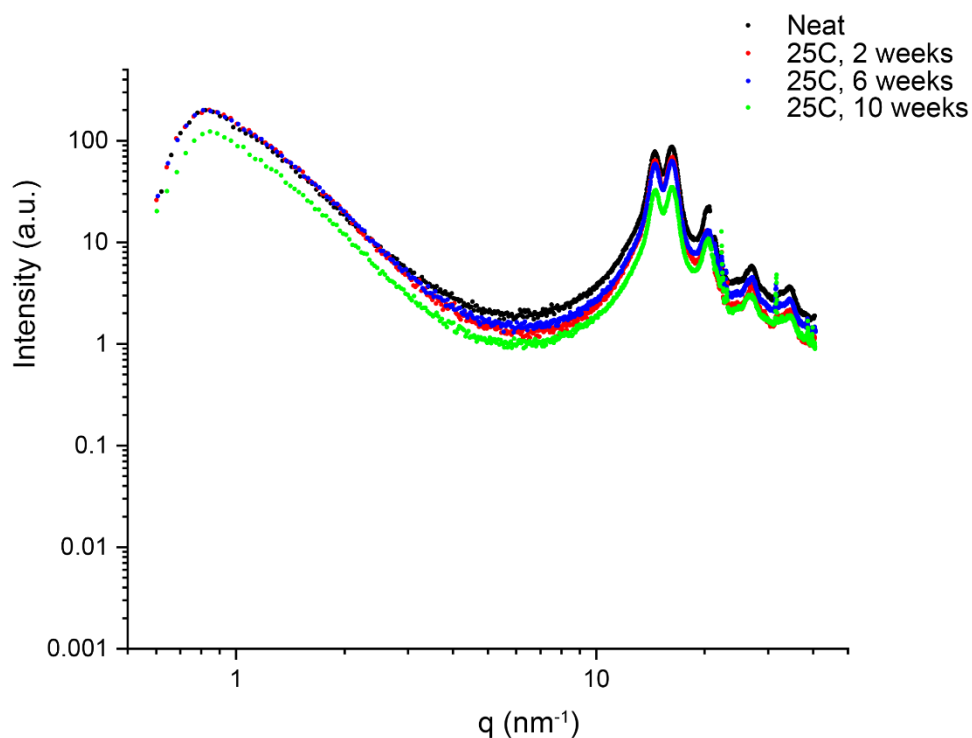
Figure 4.28 *SAXS data of PPTA fibers degraded in sweat at 25ºC.*
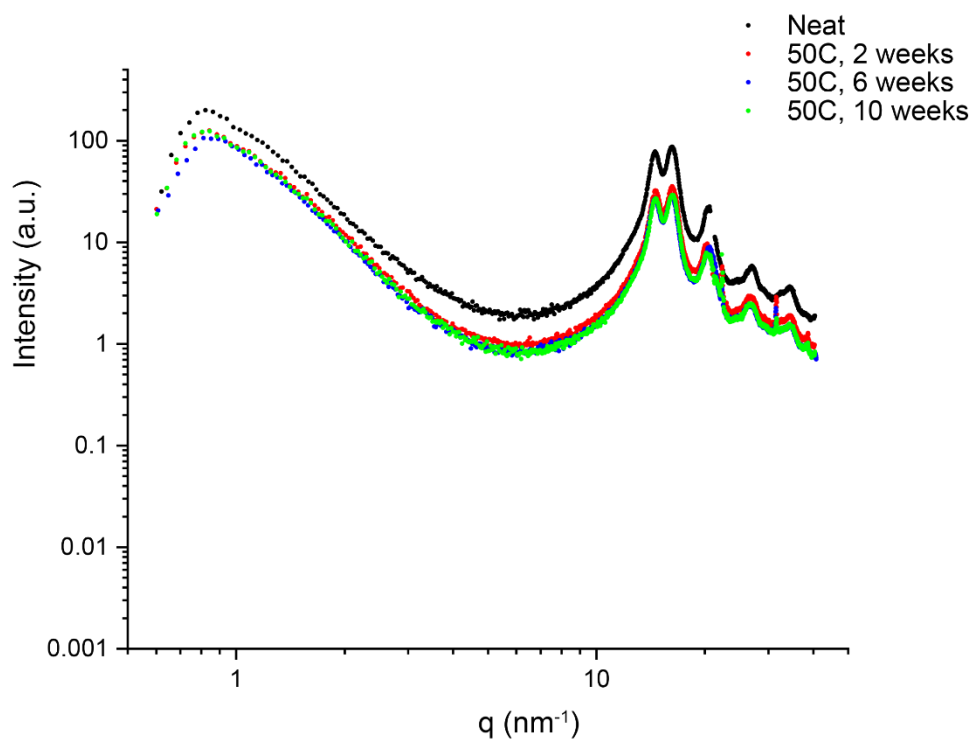
Figure 4.29 SAXS data of PPTA fibers degraded in sweat at 50°C.
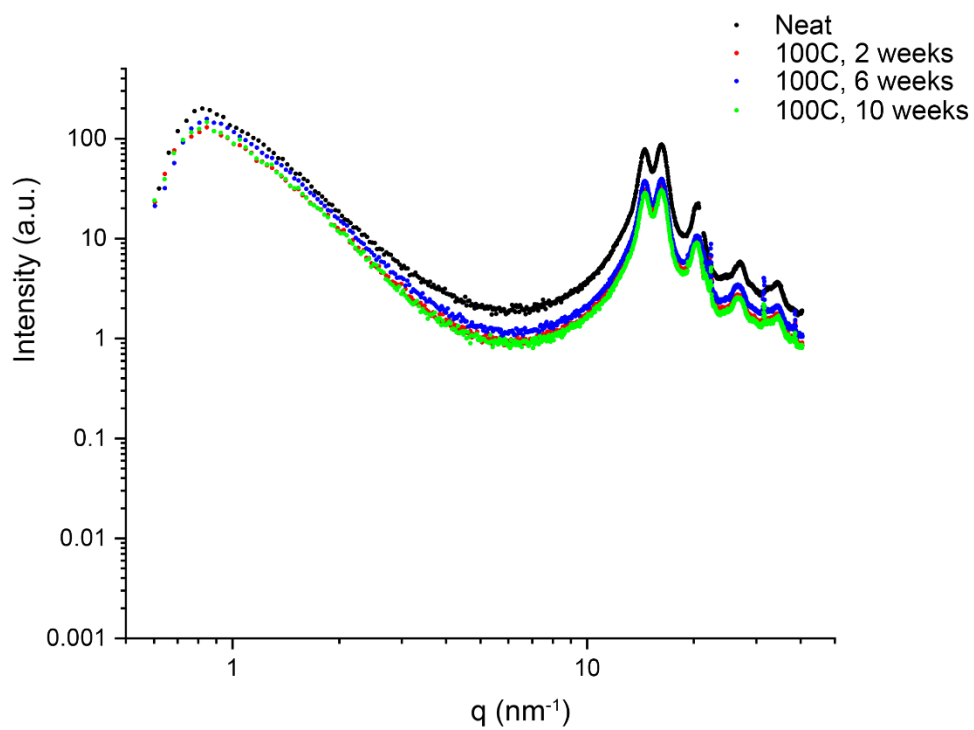
Figure 4.30 SAXS data of PPTA fibers degraded in sweat at 100°C.

SAXS is a complementary technique to PALS, and this case it has demonstrated that the saturation of PPTA fibers with acidic solutions can affect the alignment of the crystalline domain in the fibers and further decrease their mechanical performance.

4.5   **Conclusions**

It is possible to detect early stages of degradation of highly crystalline polymers such as PPTA fibers using PALS. Even when there are visual indications of degradation or great changes in the performance of the fibers, PALS detects small changes in the dimension and quantity of the free volume. Although this technique seems to be effective to the detection of said features, it results should be compared with data obtained from other technique such as SAXS. On this project, we have concluded that acid solutions have greater affinity to the PPTA molecules and consequently alters the alignment of the crystalline domains within the fibers. This decreases the mechanical performance of the fibers. At higher temperatures such as $100^{\circ}C$, sweat saturates PPTA fibers and reduces their mechanical performance.

Greater decrease in the mechanical performance was noticed for fibers with overall lower intensity (more saturated) when compared to neat fibers.

Since these results are conclusive for early stages of degradation on PPTA fibers, ten weeks is a short time to make any fit that can allow the predictions of their long-time performances under pH and sweat degradation.

CHAPTER 5 H$_2$SO$_4$ DEGRADATION OF PPTA FIBERS AND COLLABORATIONS

Additional experiments that can serve as preliminary data for upcoming research were performed on PPTA fibers. One of the experiments performed was the degradation of PPTA fibers in solutions of different concentrations of sulfuric acid (H$_2$SO$_4$) for one week at 80°C. Other experiments include studies on the humidity sorption of cellulose nanocrystals (CNCs) and the interaction of hydrogen in metal alloys. For the last two experiments mentioned, Nelyan López Pérez acquired PALS data for Md Nuruddin (CNCs project) and members of the 2017-2018 and 2018-2019 Senior Design course from the department of Materials Science Engineering at Purdue University (metal alloys project).

5.1 Degradation of PPTA Fibers in Sulfuric Acid

As mentioned in chapter 1 of this thesis, since PPTA polymers are rigid rods they are dissolved in H$_2$SO$_4$ so they can be extruded to form fibers. The PPTA-H$_2$SO$_4$ solution made for fiber consists of 20% PPTA (extrusion is carried at 80°C)[78]. Mixing H$_2$SO$_4$ with water induces chain scission through hydrolysis[30][12]. Although interaction of the PPTA fibers with H$_2$SO$_4$ is unlikely to happen during the lifetime of a bulletproof vest, little is known about how low concentrations of said acid affects their free volume.

5.1.1 *Experimental*

Sample of woven material of PPTA fibers were submerged in solutions of 0.1%, 1% , and 5% of H$_2$SO$_4$ in water. Solutions were enclosed in closed and oven proof jars covered in aluminum foil. Yarns were extracted from the woven material and used for tensile testing. Woven PPTA material was used for PALS experiments.

Tensile testing was performed on PPTA yarn fibers using an MTS Instron tensile tester 100kN. A fiber grip and 1000N load was used. Yarns were ~432mm long on the gauge length and were tested on a 50mm/min rate. Duct tape was used to avoid slippage on the ends of the yarns.

Woven PPTA for PALS was pat dried and oven dried for an hour at 100°C. Each PALS run contained around a million counts to have a more precise fit through PALSfit.

5.1.2   Mechanical testing

Results of the mechanical testing showed that the tensile stress of PPTA fibers decreased as the concentration of sulfuric acid increased (**figure 5.1**). At 5% of sulfuric acid in water only ~49% of the initial strength remained in PPTA fibers after one week at 80°C. **Table 5.1** describes the percentage of tensile strength that is retained on PPTA fibers degraded sulfuric acid aqueous solutions.

Table 5.1 *Retention of the tensile strength of PPTA degraded in H_2SO_4.*

H_2SO_4 Concentration (%)	Retained strength percent (%)
0.1	85.74
1	53.45
5	48.97

PALS data on **figure 5.2** shows a decrease on the lifetime of the o-Ps as the concentration of H_2SO_4 increased. However, the intensity (**figure 5.3**) increased with the concentration of acid. The behavior of the lifetime is similar to the results for PPTA fibers degraded on pH 4 solutions of HCl in water discussed on **chapter 3**. According to the present results, there is more saturation of the voids in PPTA fibers as the concentration of acid increased. Nevertheless, higher concentrations of acid create more voids in the structure of the fibers consequently decreasing their strength. Discussion of the t-test performed on these results are discussed in the appendix. The test revealed that there is high significance in these values.
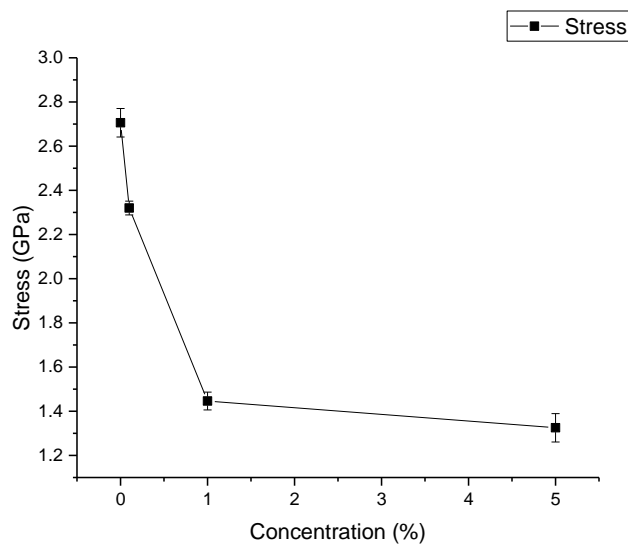
Figure 5.1 *Stress of PPTA fibers degraded in different concentrations of H_2SO_4 for one week at 80^oC.*
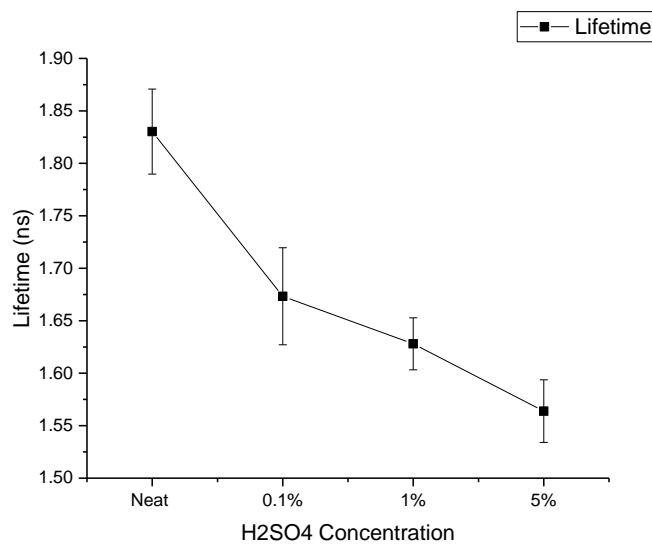
Figure 5.2 *o-Ps lifetimes of PPTA fibers degraded in solutions of different concentrations on H_2SO_4 in water at 80^oC for one week.*
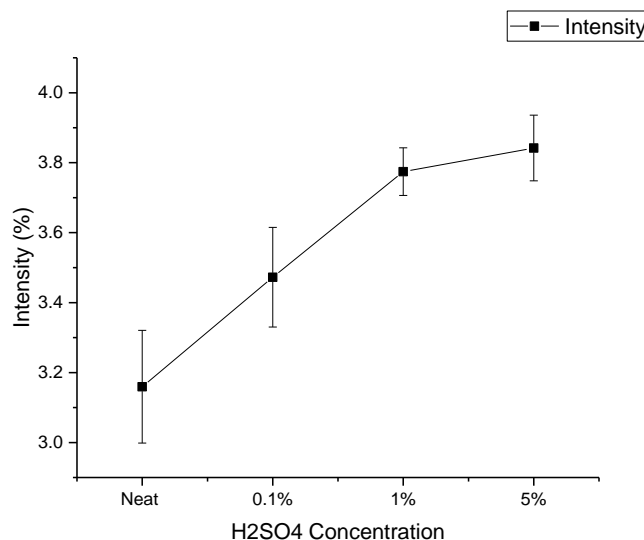
Figure 5.3 *o-Ps intensities of PPTA fibers degraded in solutions of different concentrations on H₂SO₄ in water at 80º C for one week.*

Other studies have shown a similar trend on the reduction on the mechanical properties like stress at failure and the increase of the o-Ps intensity as PPTA fibers were folded 80,000 times[48]. Moreover the decrease in tensile strength is an indicator that hydrolysis occurred and that it caused the breakage of the lateral intermolecular bonds[79]. Hence, the intensity increased as the concentration of acid increased (higher hydrolysis rate).

5.2   **Cellulose Nanocrystal Films**

CNCs are the primary structural unit of plants[80][81]. They are a renewable organic compound that are used as reinforcement in composites since the possess high tensile strength high modulus and their mechanical properties can improve depending on their alignment[81].One of the drawback of this renewable material is that it prone to water sorption, causing a decrease in the mechanical properties[46].

The cellulose molecule (**figure 5.4** [82]) is composed of hydroxyl groups that allow the hydrogen bonding and consequently promotes crystallization [83]. Like PPTA fibers, CNCs are insoluble in water and most solvents due to their high crystallinity[84], a and are rod-shaped, which indicates rigidity[80].
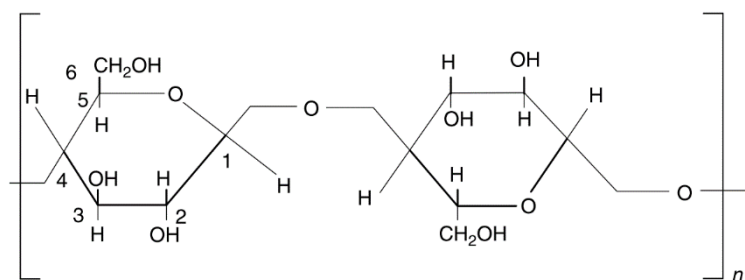
Figure 5.4 *Cellulose monomer. [9]*

A collaboration with Md Nuruddin, was made to acquire data of CNC films as they were exposed to different relative humidity. Nuruddin is currently focused on studying the sorption of CNCs depending of their alignment: chiral, aligned and random. The chiral orientation forms helical nematic structure[80][85]. On the other hand the aligned CNC films are shear oriented, while the random CNCs are not subjected to any shear stress[80].

Analyzing cellulose nanocrystal films is challenging, since the production of the films is time consuming and the final product is too thin to be used for PALS (less than 2mm in thickness). Previous studied have used crushed CNC films in a vial to be able to perform PALS at variable relative humidity and we followed their experimental setup[46].

5.2.1   Experimental

CNC films were crushed and inserted in a glass vial. Holes were made on the vial's cap. The Na^{22} source was places inside the vial and covered with CNCs. The vial was placed in a plastic bag that contained desiccant (for 0%RH) or a salt solution (90%RH). An aluminum foil ball was

used as a spacer. **Figure 5.5** is retrieved from J. Torstensen et al. and is a visual representation of the experimental setup.
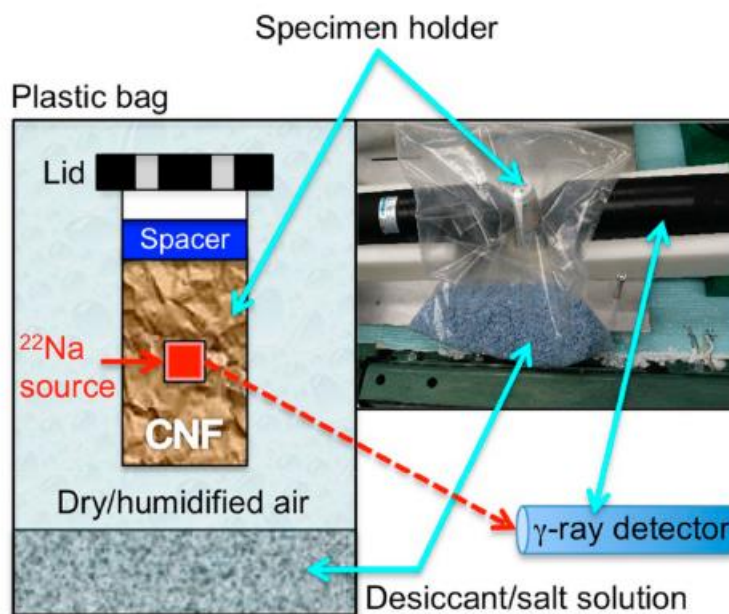
Figure 5.5 PALS setup for CNC experiements at different RH.

At the moment, PALS experiments have been performed on chiral and aligned CNCs at room RH (~50%), 0% and 90% RH. Random CNCs were tested only at room RH (~50%) and 0%RH. Both chiral and aligned CNCs were studied daily at 90%RH. Each PALS run took about a week to reach a million counts.

5.2.2 Results and discussion

Table 5.2 shows the results of the lifetime and intensity of the different CNC films at different RH. Random CNCs showed no significant change from room RH to 0%RH. On the other hand, chiral and random CNC films had similar lifetimes and intensities at room RH. At 0%RH the lifetime of chiral CNCs increased. Water was absorbed by the desiccant and removed from the CNCs. However, at 90%RH the lifetime decreased and after 7 days (when the million counts are

reached), the lifetime remains lower than at room RH and 0%RH. This means that the CNCs absorbed water during that period.

The intensity of chiral CNCs is less at 0% RH. This can be attributed to the collapse of previous voids that were occupied by water. After 7 days at 90%RH, the intensity was similar to the initial value at room RH.

It is difficult to draw conclusions from the aligned samples, when there is no data for samples at room RH. However, at 0%RH aligned CNC films had a smaller lifetime, which could be attributed to less spacing between the cellulose molecules due to alignment. After 1 day at 90%RH, the lifetime slightly decreased but instead of decreasing with time the lifetime increased after 7 days of exposure.

Table 5.2 *PALS results of random, chiral and aligned CNC films at 0% and 90%RH.*

RH (%)	Random		Chiral		Aligned	
	Lifetime (ns)	Intensity (%)	Lifetime (ns)	Intensity (%)	Lifetime (ns)	Intensity (%)
Room	1.66 ±0.012	12.91 ±0.16	1.65 ±0.012	13.61 ±0.16	---	---
0	1.67 ±0.015	11.82 ±0.21	1.83 ±0.053	8.87 ±0.77	1.66 ±0.058	10.51 ±1.13
90 (1 day)	---	---	1.321 ±0.046	15.93 ±0.94	1.62 ±0.26	10.16 ±4.77
90 (7days)	---	---	1.60 ±0.011	12.95 ±0.16	1.80 ±0.034	10.48 ±0.526

The study by J. Torstensen et al. concluded that the lo-Ps lifetime increased as humidity increases. It also concludes that saturation of the free volume occurs prior its expansion[46]. Our results suggest that saturation (lowest lifetime) for chiral and aligned CNCs at 90%RH occurred in as early as 1 day. The lifetime increased with time of exposure, which is an indicator of expansion. Greater expansion is seen in chiral CNCs than in the aligned CNCs. Also, the intensity of the chiral CNCs at 90%RH decreased from 15.93% to 12.95% was due to the presence of water in the free volume. Aligned CNCs showed little to no change in the intensity. Overall, the aligned CNCs showed to be more stable when exposed to moisture. Alignment causes organized hydrogen bonding and higher degrees of crystallinity, which prevents the interaction with water and other chemicals. High orientation and crystallinity are characteristics that are also found in PPTA fibers, which, like discussed in previous chapters, can behave like CNC fibers when exposed to humidity.

5.3   **Hydrogen Embrittlement on Advanced High-Strength Steels**

Advanced high-strength steels (AHSS) are characterized by having high tensile strength (greater than 500 MPa), complex microstructures and high strength-ductility[86]. They are commonly used in the auto industry due to their low weight and energy absorbing structural components which reduced the impact of a crash [86]. One of the drawbacks of these steels is that they are susceptible to degradation when they are in contact with hydrogen, reducing their ductility and toughness[87].

Some of the causes of degradation in AHSS that have been identified are: the formation of hydrides, the emission of dislocations induced by hydrogen adsorption, and effects in the plasticity (hydrogen enhanced localized plasticity)[87][88][89].The processing of ASHH includes the exposure to high temperatures and hydrogen. Consequently, embrittlement due to the contact with

hydrogen may occur, since the hydrogen molecules absorbed in the surface of the AHSS and the further diffusion of the hydrogen atoms in the metal.

This project consisted in the characterization of hydrogen embrittlement in AHSS provided by ArcelorMittal. In 2017-2018 the senior design students focused on martensitic steel (similar to AreclorMittal's M1700) that is composed of 0.30%wt. C, 0.45% wt. Mn, 0.01% wt. P, 0.015% S and unknown quantities of B and Ti. The effects of hydrogen on annealed and Z-milling samples was studied through PALS. Z-milling refers to the process where the steel is flatted with 2% plastic strain.

The following academic year (2018-2019) the senior design students focused on another type of martensite (M1100) and a dual-phase (DP1180) AHSS. M1100 had a chemical composition of 0.12% wt. C, 0.45% wt. Mn, and Fe is used to balance. On the other hand, the DP1180's chemical composition consists of 0.18%wt. C, 2.4% wt. Mn, 0.6% wt. and Fe is used to balance. Both years hydrogen was introduced through atomic hydrogen charging. This type of charging diffuses hydrogen with and electrolytic cell. The AHSS samples are the cathode of the cell. Said samples are immersed in an acidic solution where a 10mA current is passed. Charged and uncharged samples where compared.

5.3.1 PALS in AHSS

For PALS studies in AHSS, only two lifetimes are considered. The shortest lifetime (τ_1) is attributed to the response of the bulk material, monovacancies or dislocation cores [87][90]. On the other hand, the longest lifetime (τ_2) is attributed to larger defects and vacancies[87][91].

5.3.2 Annealed and Z-milled M1700

Results of the PALS analysis of annealed and z-milled M1700 samples are tabulated on **table 5.3**. The increase in τ_1 from 159ps (annealed) to 161ps (z-milled) can be attributed to the

plastic deformation introduced during the milling process. Furthermore, the increase from 394ps (annealed) to 403ps (z-milled) on τ_2 is attributed to the deformation caused by milling which promotes the formation of vacancies and the merging of adjacent vacancies (coalescence).

The lifetime reduction in annealed M1700 after charging is due to the presence of hydrogen in the sample. Intensity of annealed and charged annealed samples remain unchanged. However, both the τ_1 lifetime and intensity of the Z-milled samples increased after charging. This is means that Z-milled samples are more prone to hydrogen embrittlement because there are and larger vacancies than in the annealed samples prior charging. Hydrogen promotes the formation of vacancies in Z-milled samples[87].

Table 5.3 PALS results for charged and uncharged annealed and Z-milled M1700

Annealed						
	As-Received (24 hours)		Charged (6 hours after charging)		Change in lifetime	
	τ_1	τ_2	τ_1	τ_2	τ_1	τ_2
Lifetime (ps)	159	394	146	391		
Lifetime St. Dev. (ps)	3	6	4	7	-13	-3
Intensity (%)	56.7	42.5	56.9	42.4		
Z-milled						
	As-Received (24 hours)		Charged (6 hours after charging)		Change in lifetime	
	τ_1	τ_2	τ_1	τ_2	τ_1	τ_2
Lifetime (ps)	161	403	170	410		
Lifetime St. Dev. (ps)	3	6	4	10	9	7
Intensity (%)	57.3	42.0	59.5	40.1		

5.3.3   M1100 and DP1180

Both M1100 and DP1180 have an increase in τ_1 and τ_2 lifetimes (see **table 5.4).** The increase in τ_1 after charging is attributed to the expansion of the lattice. On the other hand, the increase in τ_2 after charging indicate that the voids and defects have enlarged. Since the change in

lifetime from uncharged to charge was greater for the M1100 sample, it was concluded that it was more prone to hydrogen embrittlement than DP1180. The students attribute PALS results of the M1100 to the presence of areas of inclusion in the sample, which act as hydrogen trapping sites.

Table 5.4 PALS results for charged and uncharged M1100 and DP1180.

AHSS	Lifetime (ps)		Change in Lifetime (ps)	
	τ_1	τ_2	τ_1	τ_2
Uncharged M1100	132.0	371.3	6.3	5.0
Charged M100	138.3	376.3		
Uncharged DP1180	145.5	390.6	4.4	4.5
Charged DP1180	147.9	395.1		

5.4 Conclusions

PALS is a versatile technique that can be used to measure changes in the structure of a great variety of materials. Some of the challenges that can be studied why PALS are the degradation of highly crystalline fibers like PPTA Twaron fibers, the response to humidity of CNC films, and the hydrogen embrittlement of AHSS.

Highly crystalline fibers, such as PPTA are very resistant to chemical attacks and therefore they degrade at a slow rate. Accelerating their degradation through a combination of H_2SO_4 and temperature show that higher concentrations of acid initiate the formation of more free volume leading to loss of mechanical performance. The ultimate tensile strength is greatly affected by the presence of voids and defects. The increment on the quantity of free volume in the fibers was detected due to an increase in the intensity of the lifetime of the o-Ps as the H_2SO_4 concentration increased. The information obtained through this data will be useful to study other fibers and will serve as a baseline to make predictions on the lifetime body armors.

Compared to the fibers degraded in sweat and pH 4 aqueous solutions discussed in the previous chapters, H_2SO_4 interacts with the PPTA molecules and initiates hydrolysis at a higher rate. This is because the pH of H_2SO_4 is lower than that of the HCl used for the pH 4 aqueous solution. There is more H^+ in sulfuric acid and the there is also the presence of O. The chemical composition and the size of the molecules contribute to the reduction in the lifetime of o-Ps.

On the other hand, PALS can be used to detect the swelling effect in other crystalline materials, like CNCs. CNCs have a similar behavior to PPTA fibers, since they saturate and expand as they are exposed to humidity for a long period of time. Alignment is also important on how the material is affected by humidity. Aligned CNCs are less affected by humidity.

PALS is a useful tool for the detection of hydrogen embrittlement on AHSS. The implementation of this non-destructive characterization method on AHSS can be useful on the prediction of failure under different conditions.

Overall, the use of PALS, along with mechanical testing methods, can be used on different materials to measure small changes in their physical structure and how this changes alter the performance of a material.

APPENDIX

T-test of PPTA Fibers Degraded in DI water, pH 4 and pH 10

A two-tail t-test was performed with a significance level of α=0.05 was performed. **Table 6.1** shows that all the p values of the ultimate tensile strength are significant when the values at 2 weeks are compared to the values at 10 weeks.

Table 5.5 *Results of the t-test of the tensile tests performed on the PPTA yarns degraded in DI water, pH 4, and pH 10. This table only included the t-test for the ultimate tensile strength. Values in yellow indicate significance.*

Temperature	Weeks	p-value
DI water		0.012955711
pH 4	2 &10	5.61012E-09
pH 10		0.047351

T-test of PPTA Fibers Degraded in Sweat

As in section 6.1, a t-test was performed on the results for the tensile test of the yarns degraded in sweat. A two-tail t-test with a significance level of α=0.05 was performed. **Table 6.2** shows the p values for the ultimate tensile strength of the yarns degraded in sweat at different temperatures and compared the data at 2 weeks to that obtained at 10 weeks at each temperature.

The results of the t-test indicate significance for the yarns degraded at 50ºC and 100ºC. However, the PPTA yarns degraded at 25ºC had ~21% chance of randomness.

Table 5.6 *Results of the t-test of the tensile tests performed on the PPTA yarns degraded in sweat at differen temperatures.This table only included the t-test for the ultimate tensile strength. Values in yellow indicate significance.*

Temperature	Weeks	p-value
25		0.214704
50	2 &10	0.041271
100		3.74614E-05

T-test of PPTA Fibers Degraded H_2SO_4

      The same t-test as describe on sections 6.1 and 6.2 was performed on the results of the ultimate tensile strength of PPTA yarns degraded in H_2SO_4. The p-vales are shown on **table 6.3** and reveal that the valued obtained are highly significant and not due to randomness. The results were compared to the values of neat PPTA fibers.

Table 5.7 *Results of the t-test of the tensile tests performed on the PPTA yarns degraded in aqueous solutions of different concentrations of H_2SO_4.This table only included the t-test for the ultimate tensile strength. Values in yellow indicate significance.*

H_2SO_4 Concentration (%)	p-value
0.1	3.53327E-05
1	6.72078E-14
5	7.96916E-16

REFERENCES

[1]   N. Lopez Perez, "Degradation of high performance polymeric fibers: Effects of sonication, humidity and temperature on poly (p-phenylene terephthalamide)," Purdue University, 2016.

[2]   D. Ahmed, Z. Hongpeng, K. Haijuan, L. Jing, M. Yu, and Y. Muhuo, "Microstructural Developments of Poly (p-phenylene terephthalamide) Fibers During Heat Treatment Process : A Review," *Mater. Researh*, vol. 17, no. 5, pp. 1180–1200, 2014.

[3]   T. Tam and A. Bhatnagar, "High-performance ballistic fibers and tapes," *Light. Ballist. Compos. Mil. Law-Enforcement Appl. Second Ed.*, pp. 1–39, 2016.

[4]   S. Rebouillat, "Aramids," in *High-Performance Fibers*, J. W. S. Hearle, Ed. Woodhead Publishing Limited, 2001, pp. 23–61.

[5]   N. Mao, "High performance textiles for protective clothing," in *High Performance Textiles and their Applications*, Woodhead Publishing Limited, 2014, pp. 91–143.

[6]   O. L. Shanmugasundaram, *Smart and intelligent textiles*. Woodhead Publishing Limited, 2008.

[7]   R. J. Young and P. A. Lovell, *Introduction to Polymers*, 3rd ed. Boca Raton, FL: CRC Press, 2011.

[8]   L. C. Sawyer, R. T. Chen, M. G. Jamieson, I. H. Musselman, and P. E. Russell, "The fibrillar hierarchy in liquid crystalline polymers," *J. Mater. Sci.*, vol. 28, no. 1, pp. 225–238, 1993.

[9]   I. Khoo, "Introduction to Liquid Crystals," in *Liquid Crystals*, 2nd ed., John Wiley & Sons, Inc., 2007, pp. 1–21.

[10]   R. A. L. Jones, *Soft Condensed Matter*. Oxford University Press, 2002.

[11] Teijin, "Twaron – a versatile high-performance fiber," p. 12, 2012.

[12] R. J. Morgan, C. Pruneda, and W. J. Steele, "The Relationship between the Physical Structure and the Microscopic Deformation and Failiure Processes of Poly(p-Phenylene Terephthalamide) Fibers," *J. Polym. Sci. Polym. Phys. Ed.*, vol. 21, pp. 1757–1783, 1983.

[13] D. A. Mooney and J. M. D. MacElroy, "Differential water sorption studies on Kevlar 49 and as-polymerised poly (p-phenylene terephthalamide): Adsorption and desorption isotherms," *Chem. Eng. Sci.*, vol. 59, no. 11, pp. 2159–2170, 2004.

[14] M. S. Division, "Moisture uptake by Kevlar fibres," vol. 12, pp. 60–62, 1993.

[15] H. H. Yang, *Kevlar Aramid Fiber*. West Sussex, England: John Wiley & Sons, Inc., 1993.

[16] M. Fukuda, M. Ochi, M. Miyagawa, and H. Kawai, "Moisture Sorption Mechanism of Aromatic Polyamide Fibers: Stoichiometry of the Water Sorbed in Poly(para-phenylene Terephthalamide) Fibers," *Text. Res. J.*, vol. 61, no. 11, pp. 668–680, 1991.

[17] D. A. Mooney and J. M. D. Macelroy, "Differential water sorption studies on Kevlar 49 and as-polymerized poly(p-phenylene terephthalamide): Determination of water transport properties," *Langmuir*, vol. 23, no. 23, pp. 11804–11811, 2007.

[18] J. Z. Wang, D. A. Dillard, and T. C. Ward, "Temperature and stress effects in the creep of aramid fibers under transient moisture conditions and discussions on the mechanisms," *J. Polym. Sci. Part B Polym. Phys.*, vol. 30, no. 12, pp. 1391–1400, 1992.

[19] C. Moosbrugger and A. S. M. International, "Representation of Stress-Strain Behavior," no. Eq 3, pp. 1–19.

[20] W. D. Callister, *Materials Science and Engineering : An Introduction*. John Wiley & Sons, Inc., 2007.

[21]   A. S. Argon, *The Physics of Deformation and Fractures of Polymers*. Cambrige Solid State Science Series, 2013.

[22]   J. W. S. Hearle, "Forms of fibre fracture," in *FIBER FRACTURE*, Elsevier Science Ltd., 2002, pp. 57–71.

[23]   T. Kelen, *Polymer Degradation*. Van Nostrand Reinhold Company, 1983.

[24]   R. Piazza, *Soft Matter: The Stuff that Dreams are Made of*. Milan, Italy: Springer, 2010.

[25]   R. R. Mather and R. H. Wardman, *The Chemistry of Textile Fibers*. RSC Publishing, 2011.

[26]   J. R. Fried, *Polymer Science and Technology*. 2003.

[27]   N. G. McCrum, C. P. Buckley, and C. B. Bucknall, *Principles Of Polymer Engineering.*, 2nd ed. 1997.

[28]   B. S. Mercer, "Molecular Dynamics Modeling of PPTA Crystals in Aramid Fibers," 2016.

[29]   R. J. Ouellette and J. D. Rawn, *Properties of Organic Compounds*. Elsevier Inc., 2015.

[30]   C. Arrieta, É. David, P. Dolez, and T. Vu-Khanh, "Hydrolytic and photochemical aging studies of a Kevlar-PBI blend," *Polym. Degrad. Stab.*, vol. 96, no. 8, pp. 1411–1419, 2011.

[31]   C. S. Li, M. S. Zhan, X. C. Huang, H. Zhou, and Y. Li, "Hydrothermal aging mechanisms of aramid fibers via synchrotron small-angle X-ray scattering and dynamic thermal mechanical analysis," *J. Appl. Polym. Sci.*, vol. 128, no. 2, pp. 1291–1296, 2013.

[32]   R. A. Auras, "Solubility of gases and vapors in crosslinked polymers," in *Themodynamics, Solubility and Environmental Issues*, T. M. Letcher, Ed. Elsevier B.V., 2007, pp. 343–368.

[33]   Y. Yu, "Positron Annihilation Lifetime Spectroscopy Studies of Amorphous and Crystalline Molecular Materials," no. 1, p. 115, 2011.

[34] G. Dlubek, M. Q. Shaikh, R. Krause-Rehberg, and M. Paluch, "Effect of free volume and temperature on the structural relaxation in polymethylphenylsiloxane: A positron lifetime and pressure-volume-temperature study," *J. Chem. Phys.*, vol. 126, no. 2, 2007.

[35] D. W. Van Krevelen, "Volumetric Properties," in *Properties of Polymers*, 4th ed., Elsevier Science, 2009, pp. 71–108.

[36] Y. C. Jean, P. E. Mallon, and D. M. Schrader, "Introduction to Positron and Positronium Chemistry," in *Principles and Applications of Positron and Positronium Chemistry*, River Edge, NJ: World Scientific, 2003, pp. 1–15.

[37] Y. C. Jean, J. D. Van Horn, W. S. Hung, and K. R. Lee, "Perspective of positron annihilation spectroscopy in polymers," *Macromolecules*, vol. 46, no. 18, pp. 7133–7145, 2013.

[38] R. Krause-Rehberg and H. S. Leipner, *Positron Annihilation in Semiconductors: Defect Studies*. Berlin: Springer, 1999.

[39] R. Krause-rehberg, "Fundamentals of positron annihilation spectroscopy and its application in semiconductors," *Lecture at the International School on Positron Studies*, 2009. [Online]. Available: http://positron.physik.uni-halle.de/talks/ICPA-15_ISPS_lecture_RKR.pdf.

[40] Y. C. Jean, "Positron annihilation spectroscopy for chemical analysis: A novel probe for microstructural analysis of polymers," *Microchem. J.*, vol. 42, no. 1, pp. 72–102, 1990.

[41] D. M. Bigg, "A review of positron annihilation lifetime spectroscopy as applied to the physical aging of polymers," *Polym. Eng. Sci.*, vol. 36, no. 6, pp. 737–743, 1996.

[42] P. Winberg, M. Eldrup, and F. H. J. Maurer, "Free volume dilatation in polymers by ortho-positronium," *J. Chem. Phys.*, vol. 136, no. 24, 2012.

[43] R. Ramani and C. Ranganathaiah, "Degradation of acrylonitrile-butadiene-styrene and polycarbonate by UV irradiation," *Polym. Degrad. Stab.*, vol. 69, no. 3, pp. 347–354, 2000.

[44] K. S. Liao *et al.*, "Determination of free-volume properties in polymers without orthopositronium components in positron annihilation lifetime spectroscopy," *Macromolecules*, vol. 44, pp. 6818–6826, 2011.

[45] K.-L. Tung *et al.*, "Characterization of multilayer nanofiltration membranes using positron annihilation spectroscopy," *J. Memb. Sci.*, vol. 343, no. 1–2, pp. 147–156, 2009.

[46] J. Torstensen *et al.*, "Swelling and Free-Volume Characteristics of TEMPO-Oxidized Cellulose Nanofibril Films," *Biomacromolecules*, vol. 19, no. 3, pp. 1016–1025, 2018.

[47] G. Dlubek, R. Buchhold, C. Hübner, and a. Nakladal, "Water in local free volumes of polyimides: A positron lifetime study," *Macromolecules*, vol. 32, no. 7, pp. 2348–2355, 1999.

[48] J. A. Howarter, M. Liu, W. G. McDonough, C. Soles, and G. A. Holmes, "Nanostructural evidence of mechanical aging and performance loss in ballistic fibers," *J. Polym. Sci. Part B Polym. Phys.*, pp. 1711–1717, 2017.

[49] O. P. Bajpai, S. Panja, S. Chattopadhyay, and D. K. Setua, "Process-structure-property relationships in nanocomposites based on piezoelectric-polymer matrix and magnetic nanoparticles," in *Manufacturing of Nanocomposites with Engineering Plastics*, 1st ed., 2015.

[50] C. Riekel, "Applications of micro-SAXS/WAXS to study polymer fibers," *Nucl. Instruments Methods Phys. Res. Sect. B Beam Interact. with Mater. Atoms*, vol. 199, pp. 106–111, 2003.

[51]   S. Ran *et al.*, "Studies of the mesophase development in polymeric fibers during deformation by synchrotron SAXS/WAXD," *J. Mater. Sci.*, vol. 36, no. 13, pp. 3071–3077, 2001.

[52]   M. Gazzano *et al.*, "Structure-morphology correlation in electrospun fibers of semicrystalline polymers by simultaneous synchrotron SAXS-WAXD," *Polym. (United Kingdom)*, vol. 63, pp. 154–163, 2015.

[53]   AMETEK, "Experiment 27 Positron Annihilation Lifetime Spectrometry," Oak Ridge, TN.

[54]   E. & I. P. Ziegler, "Eckert & Ziegler Reference & Calibration Sources Table of Contents." [Online]. Available: https://www.ezag.com/fileadmin/user_upload/isotopes/isotopes/Isotrak/isotrak-pdf/Product_literature/EZIPL/EZIP_catalogue_reference_and_calibration_sources.pdf.

[55]   N. J. Kirkegaa, Peter , Olsen Jens V , Eldrup, Morten , Pederson, "PALSfit: A computer program for analysing positron lifetime spectra," .

[56]   J. V Olsen, P. Kirkegaard, N. J. Pedersen, and M. Eldrup, "PALSfit : A new program for the evaluation of positron lifetime spectra," vol. 4006, no. 10, pp. 4004–4006, 2007.

[57]   Y. G. Adewuyi, "Sonochemistry : Environmental Science and Engineering Applications," *Eng. Chem. Res.*, vol. 40, pp. 4681–4715, 2001.

[58]   I. Masselin, X. Chasseray, L. Durand-Bourlier, J. M. Lainé, P. Y. Syzaret, and D. Lemordant, "Effect of sonication on polymeric membranes," *J. Memb. Sci.*, vol. 181, no. 2, pp. 213–220, 2001.

[59]   A. Tomljenović and R. Čunko, "Reducing Fibrillation Tendency of Man-made Cellulose Fibres Employing Ultrasound Treatment," *J. Text. Inst.*, vol. 95, no. 1, pp. 327–339, 2004.

[60] K. Iyer, R.V. , Vijayan, "Ultrasonic Agitation of Kevlar Fibres," *Curr. Sci.*, vol. 71, no. 5, pp. 398–400, 1996.

[61] R. Edmunds and M. A. Wadee, "On kink banding in individual PPTA fibres," *Compos. Sci. Technol.*, vol. 65, no. 7–8, pp. 1284–1298, 2005.

[62] M. Andrassy and E. Pezelj, "Reduction of Aging Tendency in p-Aramide Fibers," pp. 2340–2345, 1999.

[63] ASTM, "Standard Test Method for Tensile Properties of Yarns by the Single-Strand Method," *ASTM Int.*, vol. D2256/D225, no. 10, pp. 1–13, 2015.

[64] M. Fukuda, M. Ochi, M. Miyagawa, and H. Kawai, "Moisture Sorption Mechanism of Aromatic Polyamide Fibers: Stoichiometry of the Water Sorbed in Poly(para-phenylene Terephthalamide) Fibers," *Text. Res. J.*, vol. 61, no. 11, pp. 668–680, 1991.

[65] W. E. Morton and J. W. S. Hearle, "Theories of moisture sorption," in *Physical Properties of Textile Fibres*, 4th ed., 2008.

[66] M. G. Dobb, D. J. Johnson, and B. P. Saville, "Supramolecular structure of a high-modulus polyaromatic fiber (Kevlar 49)," *J. Polym. Sci. Polym. Phys. Ed.*, vol. 15, pp. 2201–2211, 1977.

[67] X. Li *et al.*, "In situ synchrotron small- and wide-angle X-ray study on the structural evolution of Kevlar fiber under uniaxial stretching," *RSC Adv.*, vol. 6, no. 85, pp. 81552–81558, 2016.

[68] P. K. Gupta, *Fiber Fracture*. Elsevier Science Ltd., 2002.

[69] H. H. Yang, "Aramid fibers," in *Comprhensive Composite Materials*, 2000, pp. 199–229.

[70] J. Chin, S. Petit, A. Forster, M. Riley, and K. Rice, "Effect of Artificial Perspiration and Cleaning Chemicals on the Mechanical and Chemical Properties of Ballistic Materials *," vol. 113, pp. 567–584, 2009.

[71] A. Abu Obaid, J. M. Deitzel, J. W. Gillespie, and J. Q. Zheng, "The effects of environmental conditioning on tensile properties of high performance aramid fibers at near-ambient temperatures," *J. Compos. Mater.*, vol. 45, no. 11, pp. 1217–1231, 2011.

[72] A. D. English, "Microscopic Dynamics and Macroscopic Mechanical Deformation of Poly(pphenyleneterephtha1amide) Fibers," pp. 1152–1158, 1995.

[73] C. L. Jackson *et al.*, "Dynamic structure and aqueous accessibility of poly (p-phenylene terephthalamide) crystallites *," vol. 35, no. 6, pp. 1123–1131, 1994.

[74] R. J. Schadt, E. J. Cain, K. H. Gardner, V. Gabara, S. R. Allen, and A. D. English, "Terephthalamide Ring Dynamics of Polyip-phenyleneterephthalamide)*," pp. 6503–6508, 1993.

[75] R. J. Morgan and C. O. Pruneda, "The characterization of the chemical impurities in Kevlar 49 fibres," *Polymer (Guildf).*, vol. 28, no. 2, pp. 340–346, 1987.

[76] Y. Rao, A. J. Waddon, and R. J. Farris, "Structure-property relation in poly(p-phenylene terephthalamide) (PPTA) fibers," *Polymer (Guildf).*, vol. 42, no. 13, pp. 5937–5946, 2001.

[77] R. J. Young, D. Lu, R. J. Day, W. F. Knoff, and H. A. Davis, "Relationship between structure and mechanical properties for aramid fibres," *J. Mater. Sci.*, vol. 27, no. 20, pp. 5431–5440, 1992.

[78] R. J. Morgan and N. L. Butler, "Hydrolytic degradation mechanism of Kevlar 49 fibers when dissolved in sulfuric acid," *Polym. Bull.*, vol. 27, no. 6, pp. 689–696, 1992.

[79] L. Yu. Yu, H. M. Shen, and Z. L. Xu, "Degradation of Aramid Fibers Under Alkaline and Neutral Conditions: Relations Between the Chemical Characteristics and Mechanical Properties," *J. Appl. Phys.*, vol. 113, pp. 1763–1772, 2009.

[80] J. A. Diaz, X. Wu, A. Martini, and R. J. Moon, "Thermal Expansion of Self-Organized and Shear-Oriented Cellulose Nanocrystal Films," 2013.

[81] M. C. Valone, "EFFECT OF HUMIDITY ON THE CREEP RESPONSE OF CELLULOSE NANOCRYSTALS FILMS A," Purdue University, 2016.

[82] W. Y. Hamad, "Assembly and Structure in Native Cellulosic Fibers," in *Cellulose Nanocrystals: Properties, Production and Applications*, 1st ed., John Wiley & Sons Ltd., 2017, pp. 16–32.

[83] W. Y. Hamad, "Properties of Cellulose Nanocrystals," in *Cellulose Nanocrystals: Properties, Production and Applications*, 1st ed., John Wiley & Sons Ltd., 2017, pp. 65–137.

[84] J. Tang, J. Sisler, N. Grishkewich, and K. C. Tam, "Functionalization of cellulose nanocrystals for advanced applications," *J. Colloid Interface Sci.*, vol. 494, pp. 397–409, 2017.

[85] H. Wan *et al.*, "Rapidly Responsive and Flexible Chiral Nematic Cellulose Nanocrystal Composites as Multifunctional Rewritable Photonic Papers with Eco-Friendly Inks," 2018.

[86] M. Y. Demeri, "Advanced High-Strength Steels," in *Advanced High-Strength Steels-Science, Technology, and Applications*, ASM International, 2013.

[87] S. K. Lawrence *et al.*, "Effects of grain size and deformation temperature on hydrogen-enhanced vacancy formation in Ni alloys," *Acta Mater.*, vol. 128, pp. 218–226, 2017.

[88]   S. P. Lynch, "Mechanisms of environmentally assisted cracking in AlZnMg single crystals," *Corros. Sci.*, vol. 22, no. 10, pp. 925–937, 1982.

[89]   H. K. Birnbaum and P. Sofronis, "Hydrogen-enhanced localized plasticity--a mechanism for hydrogen- related fracture," *Mater. Sci. Eng.*, vol. 176, pp. 191–202, 1994.

[90]   E. E. Abdel-Hady, "Positron annihilation lifetime study of irradiated and deformed low density polyethylene," *Polym. Degrad. Stab.*, vol. 80, no. 2, pp. 363–368, 2003.

[91]   H. Ohkubo, Z. Tang, Y. Nagai, M. Hasegawa, T. Tawara, and M. Kiritani, "Positron annihilation study of vacancy-type defects in high-speed deformed Ni, Cu and Fe," *Mater. Sci. Eng. A*, vol. 350, no. 1–2, pp. 95–101, 2003.